ISSN 2079-9780, Review Journal of Chemistry, 2016, Vol. 6, No. 1, pp. 49–82. © Pleiades Publishing, Ltd., 2016

Copper-Containing Enzymes: Site Types and Low-Molecular-Weight Model Compounds

K. I. Tishchenko*, E. K. Beloglazkina, A. G. Mazhuga, and N. V. Zyk

Faculty of Chemistry, Moscow State University, Moscow, 119991 Russia

**e-mail: ktishchenko@mail.ru*

Received September 30, 2015; in final form, October 8, 2015

Abstract—A structured description is suggested for the existing types of copper-containing sites in copper proteins. The most important specific features of mono-, di-, tri-, and tetranuclear sites are reported, and the structural geometry of each site is considered. The functional features and catalytic reactions characteristics of each type of site are discussed. Examples of copper-containing enzyme mimics are considered, and the importance of their synthesis and use is demonstrated.

Keywords: types of copper-containing enzymes, small blue proteins (cupredoxins), "blue" oxidases, "nonblue" oxidases, type 1, type 2, type 3, type 4, Cu_A-type, Cu_B-type, Cu_Z-type, low-molecular-weight models, mimics.

DOI: 10.1134/S2079978016010027

Contents

1. INTRODUCTION

Copper is an essential trace element contained in many vitamins, hormones, enzymes, and respiratory pigments, and it is involved in metabolic processes and tissue respiration. Copper is of great significance for maintaining the normal structure of bones, cartilages, and tendons (collagen) and for the elasticity of blood vessel walls, pulmonary alveoli, and skin (elastin). Copper shows pronounced anti-inflammatory properties, mitigates symptoms of autoimmune diseases (e.g., rheumatoid arthritis), and enhances iron absorption. Acting on carbohydrate metabolism, copper accelerates glucose oxidation and suppresses hepatic glycogen breakdown [1]. In addition, copper is a component of the myelin sheath of nerves. It was demonstrated that copper is an essential component of the nervous system of higher eukaryotes, being present in proteins responsible for the biosynthesis of catecholamine and peptide hormones/neurotransmitters [2]. Copper is present in the antioxidant protection system of the organism, being a cofactor of

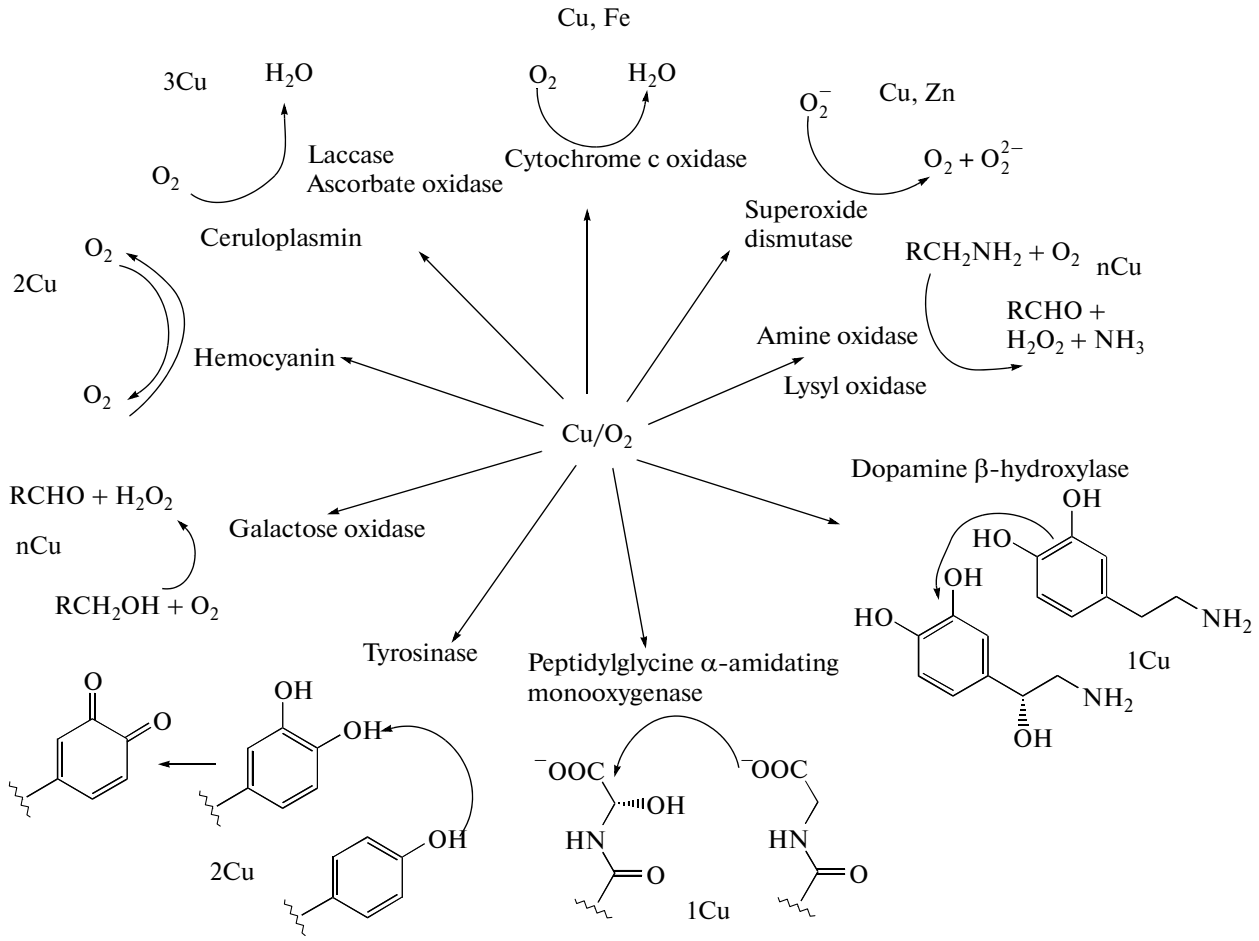

Fig. 1. Copper-containing enzymes involved in oxidation catalysis.

superoxide dismutase, which is involved in the neutralization of free radicals of oxygen, and serving as a key cofactor in various biochemical redox reactions [3].

Changes in the activity of copper-containing enzymes exert the following adverse effects: serious disorders in a number of biochemical processes, including the phospholipid, phosphatide, and heme syntheses; a large decrease in the myoglobin concentration (particularly in the cardiac muscle), in the RNA concentration in the brain, and in the glutathione concentration in the liver; a decrease in the amount of elastin and an increase in collagen solubility in the aorta and coronary arteries. The most toxic agents acting in the organism under copper deficiency conditions include sulfides. They form in the liver as a result of cysteine decomposition, accumulate as a consequence of a 2- to 3-fold decrease in the activity of sulfide oxidase, and damage the liver, and, after the barrier function of the liver is impaired, they cause damage to other organs [4].

Over 25 copper-containing enzymes are known today. The biological functions of copper-containing enzymes are associated with the following processes:

electron transfer;

oxygen binding, storage, and transport;

oxidation catalysis;

nitrous oxide reduction at the last stage of the nitrogen cycle.

These functions are due to the following specific features of copper:

Copper ions react more actively with amino acids and proteins than the ions of other vital metals, yielding more stable complexes.

Copper ions, particularly their complexes with proteins, are effective catalysts.

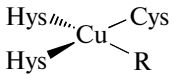

Fig. 2. General structure of type-1 enzymes.

Copper passes readily from one oxidation state to another, providing favorable conditions for its compounds to execute their redox functions. The relative stability of Cu^{+} and Cu^{2+} complexes depends on the nature of their ligand, and the $2Cu^{+} \rightarrow Cu^{2+} + Cu$ equilibrium can shift readily in either direction, depending on reaction conditions. For example, different copper-containing oxidases execute their functions through cyclic transitions between these states of copper, continuously involving dioxygen.

Figure 1 presents a number of enzymes for which one of the main functions is their interaction with oxygen [5–9].

According to the number of copper atoms in their structure, copper proteins are classified into mononuclear, dinuclear, trinuclear, and tetranuclear. The table lists copper-containing enzyme types, which differ in active site and spectral characteristics [10].

Interest in low-molecular-weight models of copper-containing enzymes is due to their high potential in the simulation of processes involving enzymes, such as catalytic reactions, oxygen transport, and electron transfer. Knowledge of the structure and properties of these models would make it possible to test them as potential drugs.

Copper complexes proved effective in the treatment of various neurodegenerative diseases, as well as in the treatment of malignant tumors, such as brain, mammary gland, and large intestine cancers, and other diseases [11]. It was also demonstrated that inorganic copper complexes can be effective in cancer therapy owing to their cytotoxic action on tumor cells [12].

Researchers focus their attention on binary copper(II) coordination compounds that are cytotoxic or capable of inhibiting enzymes, thus exhibiting their antitumor activity. A large number of dinuclear copper(II) coordination compounds considered as potential anticancer agents have been developed. Trinuclear copper(II) complexes also attract the interest of researchers. The number of copper(I) coordination compounds is incomparably smaller because of their low stability [13].

The table systematizes data concerning copper-containing enzyme types and their geometry and functions in the organism and provides examples of enzymes having the above-mentioned active sites.

2. TYPE-1 COPPER-CONTAINING ENZYMES

The enzymes with this type of active site give rise to a strong absorption band near 600 nm and are characterized by a very high redox potential (183–680 mV) and a weak hyperfine splitting in the EPR spectrum. Type 1 can be subdivided into the following groups: small blue proteins (cupredoxins), which include azurin, the plastocyanin family, the phytocyanin family (umecyanin, plantacyanin, stellacyanin),

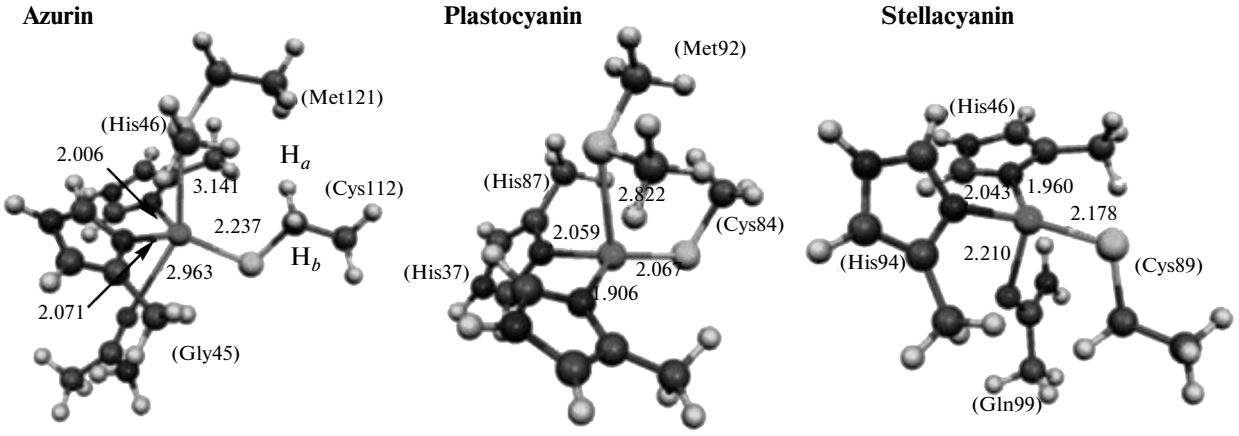

Fig. 3. Coordination of the copper ion in the active sites of azurin, plastocyanin, and stellacyanin [23].

Types of copper-containing sites

Type	Mononuclear site		
	Type 1	Type 2	$\tilde{N}u_B$
UV spectroscopy	Strong absorption band at ~600 nm and (in some proteins) 450 nm	Absorption at ~700 nm	Absorption at ~610 nm
Main ligands	His, Cys, (Met)	His, Asp, (Tyr)	His
Geometry	Distorted tetragonal Trigonal planar	Distorted tetragonal	Trigonal pyramid
Examples of structure [14, 15]	Amicyanin 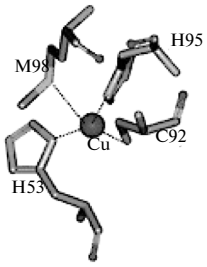	Superoxide dismutase 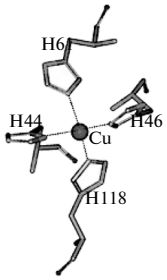	Cytochrome c oxidase 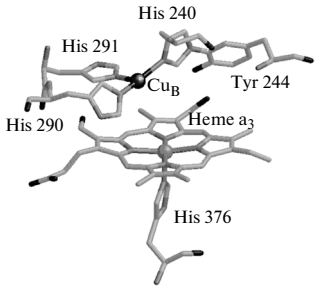
Function (catalyzed reaction)	Electron transfer	Catalysis of oxidation and reduction reactions	Oxygen transport
Examples	Plastocyanin Azurin Stellacyanin Nitrite reductase Laccase Pseudoazurin Plastocyanins Amicyanin Rusticyanin Halocyanin Sulfocyanins Umecyanin Plantacyanin Stellacyanin	Superoxide dismutase Galactose oxidase Amine oxidase Nitrite reductase Laccase	Cytochrome c oxidase
Type	Dinuclear site		
	Type 3	Cu_A	
UV spectroscopy	Absorption at ~700 nm	Strong absorption bands at ~480 and ~530–580 nm, absorption band at 800 nm	
Main ligands	His, (Tyr)	His, Cys, (Met)	
Geometry	Tetragonal	Trigonal planar	
Examples of structure [14, 16]	Hemocyanin 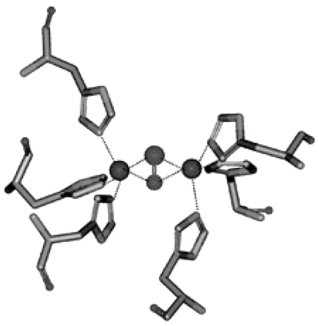	Cytochrome c oxidase, Cu_A site 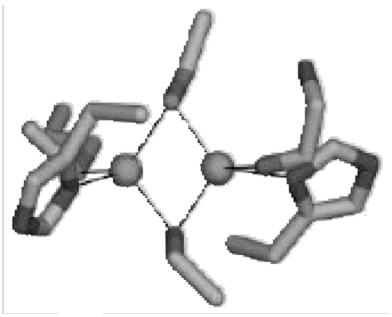	
Function (catalyzed reaction)	Amino acid oxidation Oxygen transport	Oxygen transport	
Examples	Hemocyanin Tyrosinase Catechol oxidase Laccase	Cytochrome c oxidase N_2O reductase	

Table (Contd.)

Type	Trinuclear site	Tetranuclear site
	Type 4 (Type 2 + Type 3)	Cu_Z
UV spectroscopy	Absorption at 330 and ~600 nm	Strong absorption at ~640 nm
Main ligands	His	His, S^{2-}
Geometry	Trinuclear site	$_4$-S^{2-} tetranuclear copper cluster
Examples of structure [17, 18]	Laccase from *Trametes hirsuta* (hairy bracket) 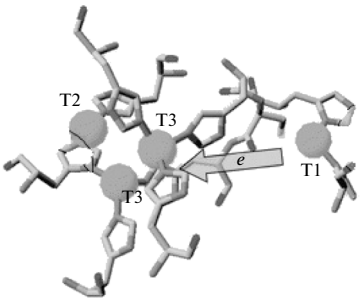	N_2O reductase from the gram-negative bacterium *Pseudomonas stutzeri* 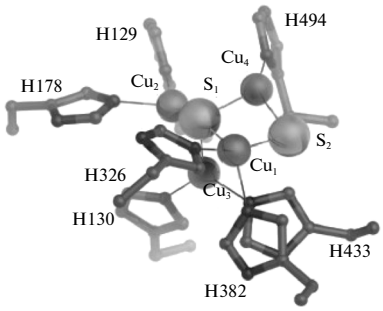
Function (catalyzed reaction)	Oxidation catalysis	Nitrous oxide reduction to molecular nitrogen
Examples	Laccase Ascorbate oxidase Ceruloplasmin	N_2O reductase

rusticyanin, auracyanin, and "blue" oxidases (ascorbate oxidase, laccase, ceruloplasmin). The general structure of type-1 enzymes is presented in Fig. 2. Blue copper proteins can contain type-1 copper sites or copper sites of all types (as in the case of blue oxidases; see the Type-1 Copper-Containing Enzymes (Type 2 + Type 3) section). The whole binding site of type-1 enzymes has the shape of an irregular tetrahedron, which is likely a compromise between the regular tetrahedral coordination characteristic of Cu^+ and the square-planar coordination typical of Cu^{2+} in low-molecular-weight copper complexes and non-blue copper-containing conjugated proteins. It is most likely that, requiring the smallest amount of energy for site reorganization, this shape allows the type-1 copper ion to pass extraordinarily rapidly from one oxidation state to another and back and, in turn, this enables the enzymes containing one or two independent type-1 sites to participate effectively in electron transfer reactions [19, 20].

2.1. Small Blue Proteins (Cupredoxins)

Small blue proteins (cupredoxins), which are water-soluble enzymes containing one copper atom, are responsible for S(Cys) Cu(II) electron transfer in the transport chain in prokaryotes and eukaryotes in the respiration and photosynthesis processes [9]. The copper atom in the active site of cupredoxins is in a distorted tetrahedral ligand environment and is coordinated by three main ligands, namely, two histidine res-

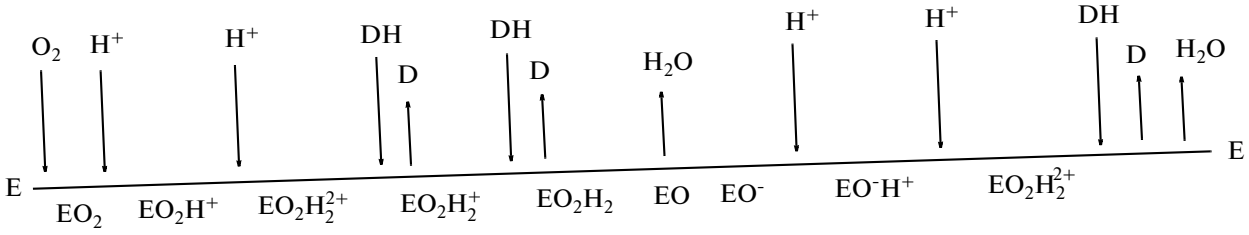

Fig. 4. Scheme of oxygen-to-water reduction catalyzed by "blue" copper-containing oxidases. EO_2 and $EO^{-}H_2^{2+}$ are possible intermediate states of the active site.

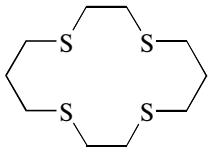

Fig. 5. Example of the symmetric structure of the thioether ligand serving as the basic element of the low-molecular-weight model of "blue" oxidases.

idues and one cysteine residue. All cupredoxins but stellacyanin have a fourth ligand (sulfur atom of methionine in the axial position). Azurin has an extra, fifth, ligand, namely, the carboxyl oxygen atom of glycine (Fig. 3) [6, 20–22].

Plastocyanin is an element of the heterooligomeric integral membrane protein complex cytochrome b_6f, which is responsible for electron transport in oxygen-evolving photosynthetic membranes [24]. In this system, the cytochrome f fragment is the electron donor, while the $P700^+$ fragment accepts an electron from the reduced plastocyanin [25].

Plastocyanin ($Cu^{2+}Pc$) is reduced by cytochrome f via the following reaction:

$$Cu^{2+}Pc + e^- \rightarrow Cu^+Pc.$$

The reduction product, Cu^+Pc, binds to the F subunit of photosystem I. P700+ oxidizes Cu + Pc via the following reaction:

$$Cu^+Pc \rightarrow Cu^{2+}Pc + e^-.$$

"Blue" oxidases are the group of enzymes responsible for the four-electron reduction of dioxygen to water without hydrogen peroxide formation as an intermediate step. This reaction includes oxygen addition and transfer of four electrons and four protons to the oxygen. When the compound undergoing oxidation (reaction substrate) is a one-electron donor, the process can be schematized by Fig. 4.

The most comprehensively studied "blue" oxidases at the moment are laccase, acsorbate oxidase, and ceruloplasmin [26]. These enzymes contain not only type-1 copper ions but also type-2 and type-3 copper ions, and it is the latter that determine their main biological role. For this reason, a more detailed description of the structure and functions of these enzymes will be presented below (see paragraph 1.4).

2.2. Examples of Low-Molecular-Weight Models of Type-1 Enzymes

Thioether complexes in which the copper atom is located in the center of a symmetric ligand (Fig. 5) were among the first low-molecular-weight analogs of "blue" oxidases to be synthesized.

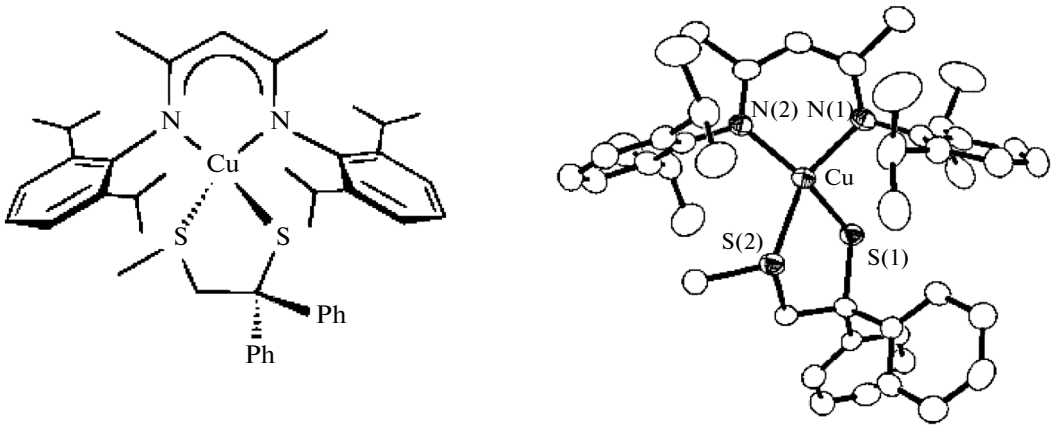

Fig. 6. Low-molecular-weight model of the "blue" oxidase laccase [28].

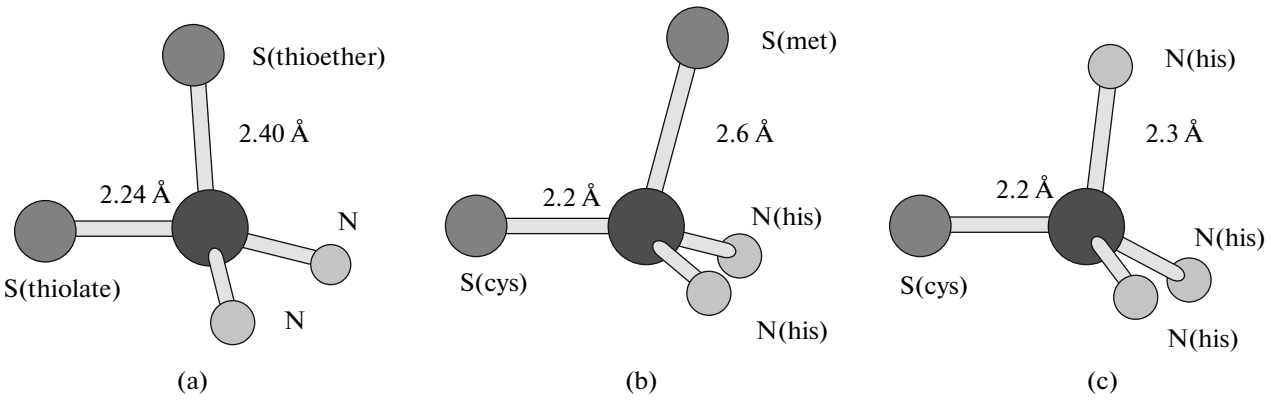

Fig. 7. Active site geometry in low-molecular-weight models of (a) laccase, (b) nitrite reductase pdb1NDT, and (c) azurin M121H [28].

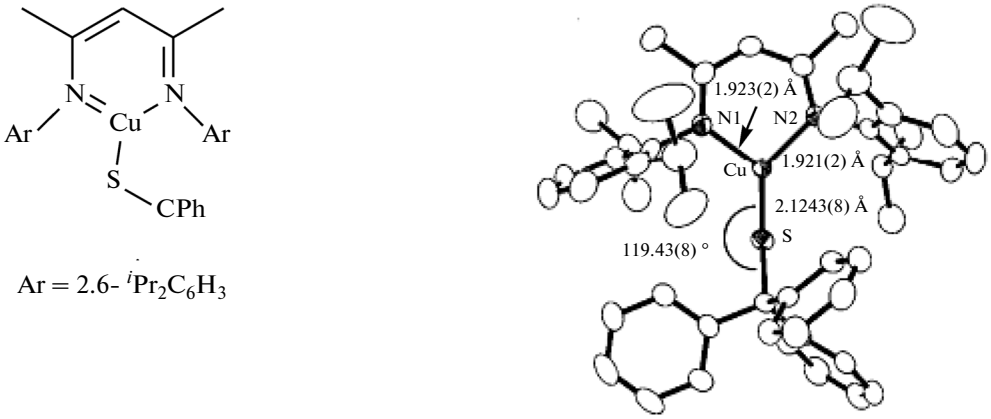

Fig. 8. Structure of the synthetic model of fungal laccase and ceruloplasmin.

These compounds are similar to enzymes not only in their spectral properties but also in their redox potentials [27]. The presence of a strong absorption band around 600 nm in the spectra of the thioethers makes them promising models for analyzing the properties of small copper proteins.

Holland and Tolman [28] developed a model of the type-1 copper site of fungal laccase (Fig. 6).

Because of slight distortion, the general geometry of the ligand differs from the "classical" geometry of the type-1 copper site but is similar to the geometry of modified azurins (e.g., M121H azurin) and nitrite reductase. In the electronic absorption spectrum of the synthesized complex, the characteristic band is markedly shifted, appearing at 691 nm, and is less intense. These spectral changes are similar to the

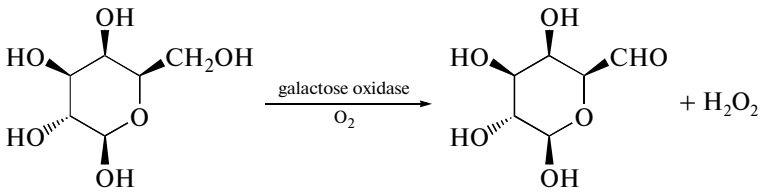

Scheme 1.

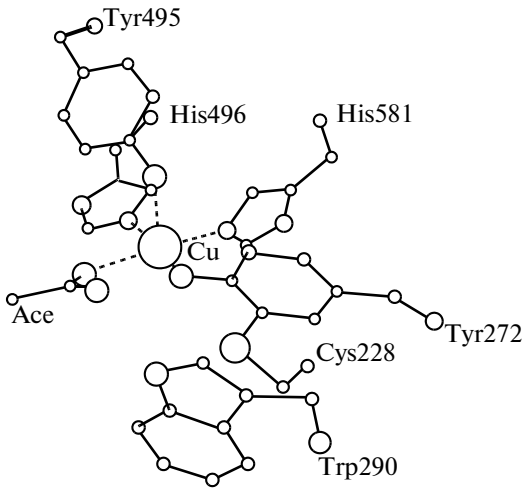

Fig. 9. Coordination of the copper ion in the active site of galactose oxidase [42].

changes caused by glutamine deprotonation in the modified azurin M121H and can be explained by an increase in the Cu–S(thiolate) bond length (Fig. 7).

The thioether residue in the model complex is strongly bonded to the copper atom. The molecular structure resulting from this coordination coincides most closely with the structure of the type-"1.5" site [29–32] and is close to trigonal planar geometry.

Holland and Tolman [33] considered a synthetic model of fungal laccase and ceruloplasmin that is structurally similar to trigonal planar geometry (Fig. 8).

The Cu–N and Cu–S bond lengths in this model (1.922 and 2.124 Å, respectively) are close to the bond lengths in the crystal structure of the trigonal planar type-1 active site of fungal laccase (1.9 and 2.2 Å, respectively). The band at $\lambda = 749$ nm in the absorption spectrum of this low-molecular-weight model in heptane indicates an intense blue color of the complex, although it occurs at a longer wavelength than the same band observed for the type-1 copper sight ($\lambda \sim 600$ nm).

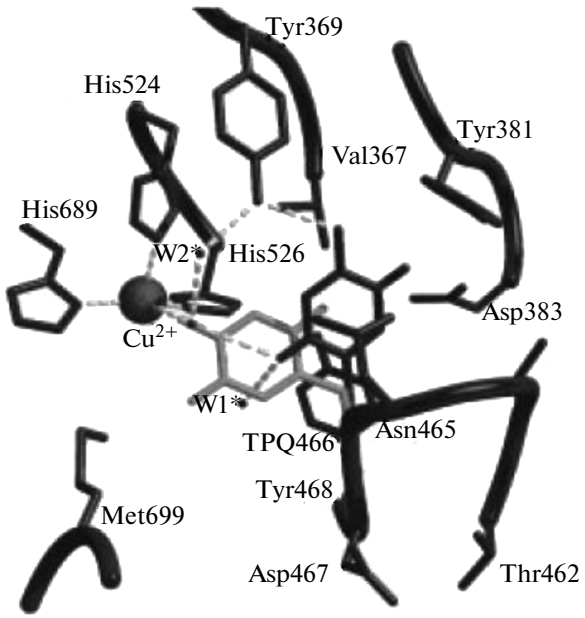

Fig. 10. Copper active site in famine oxidase [41]. In the inactive form of the enzyme, the copper atom is bonded to a modified tyrosine residue (green).

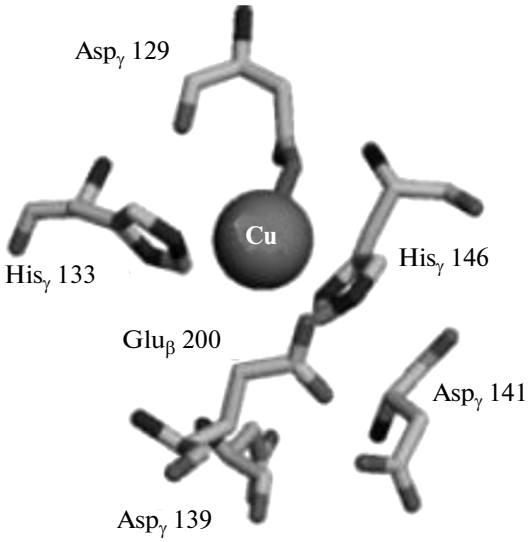

Fig. 11. Mononuclear copper site of membrane-associated methane monooxygenase pMMO from the bacterium *Methylosinus trichosporium* OB3b [49].

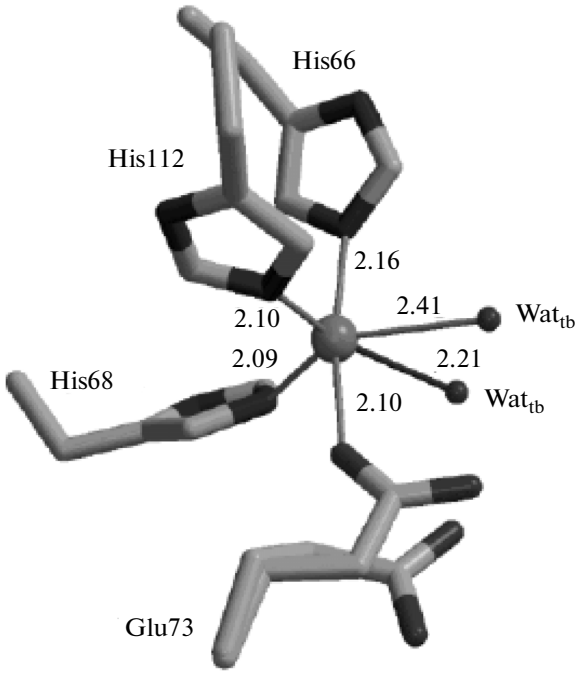

Fig. 12. Tetragonal structure of quercetin 2,3-dioxygenase and mixed trigonal bipyramidal and square pyramidal active site geometry [51].

It is supposed that the trigonal planar structure, which is unnatural for the type-1 site, minimizes the changes in the ligand upon the reduction of Cu(II) to Cu(I) [34].

3. TYPE-2 COPPER-CONTAINING ENZYMES

Type-2 enzymes, which were distinguished by EPR spectroscopy, include the following: "nonblue" oxidases (galactose oxidase and amine oxidase), oxidoreductases (monooxygenases and dioxygenases),

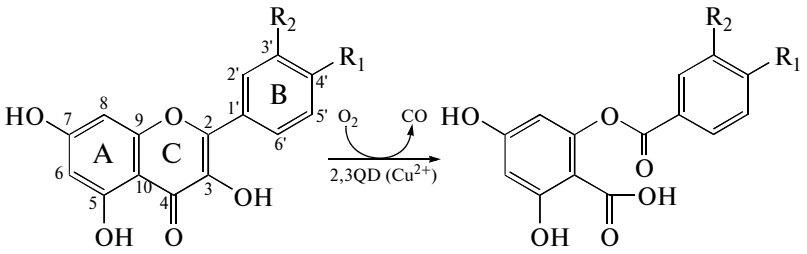

Fig. 13. Cleavage of the flavonol substrates quercetin (5,7,3',4'-tetrahydroxy flavonol, $R_1 = R_2 = OH$) and kaempferol (5,7,4'-trihydroxy flavonol, $R_1 = OH$, $R_2 = H$).

and some dinuclear enzymes (Cu–Zn superoxide dismutase) [35–37]. The enzymes of this type are characterized by "normal" EPR parameters ($g_{II} > g_{\perp} > 2.00$, $A_{II} > 140 \times 10^{-4}\,cm^{-1}$) and their visible spectrum shows a weak band [38, 39]. The copper atom in the type-2 site is in a distorted tetrahedral ligand environment.

3.1. "Nonblue" Oxidases

Copper enzymes containing a type-2 active site are referred to as "normal" or "nonblue" copper enzymes for the reason that their spectral characteristics are the same as those of common copper(II) complexes. The main function of the "nonblue" oxidases is catalysis of oxygen reduction to hydrogen peroxide. The geometry characteristic of this type of oxidase is a square planar or square pyramidal (Fig. 9) [2, 40, 41].

Galactose oxidase is an enzyme isolated from the wood-rotting fungus *Polyporus circinatus* Fr [43]. It contains one copper atom, which catalyzes the oxidation of primary alcohols into aldehydes [7, 44, 45] (Scheme 1).

Amine oxidase catalyzes the deamination of primary amines via the transfer of two electrons from the amine to dioxygen. The mechanism of this reaction can be represented as the following two consecutive steps: the first is the reduction of the enzyme by the substrate (1), and the second is the oxidation of the enzyme by oxygen (2) [6, 45]:

$$E_{ox} + R{-}CH_2{-}NH_3^+ \xrightarrow{[O]} E_{red}{-}NH_2 + R{-}CHO \quad (1)$$

$$E_{red}{-}NH_2 + O_2 \xrightarrow{[H]} E_{ox} + NH_3 + H_2O_2 \quad (2)$$

The active site of amine oxidase has the structure of a distorted square pyramid (Fig. 10). The base of the pyramid is formed by three histidine residues and a water molecule. The apex of the pyramid is another water molecule [41].

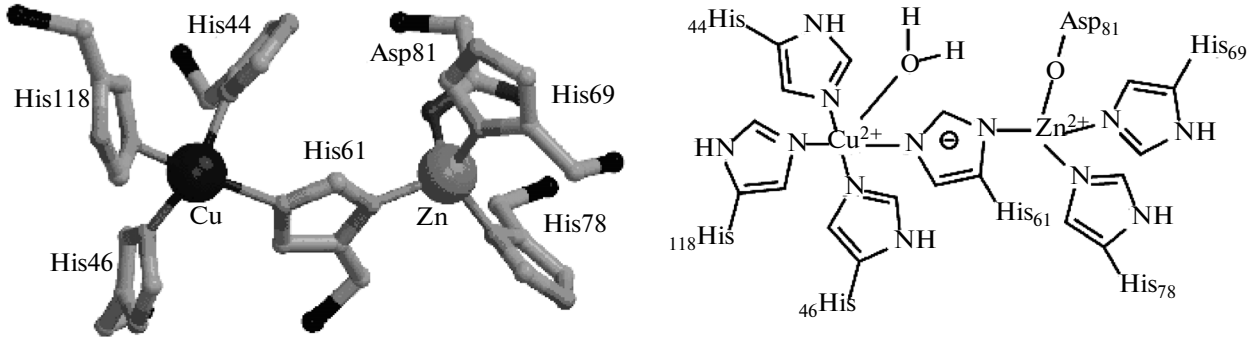

Fig. 14. Structure of the active site of Cu–Zn superoxide dismutase.

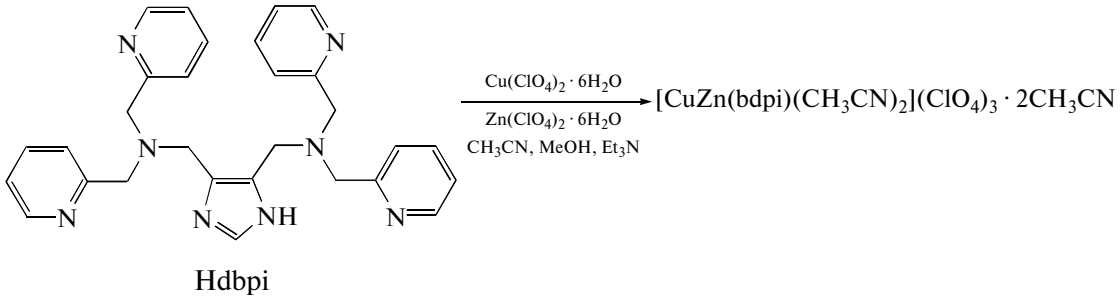

Fig. 15. Formation of the heteronuclear coordination compound containing copper and zinc ions.

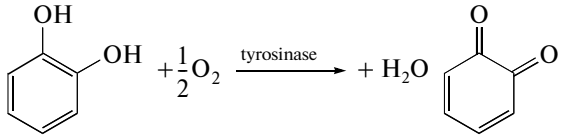

Scheme 2.

3.2. Oxyreductases

The main function of monooxygenases and dioxygenases is insertion of an oxygen atom into an organic substrate, with dioxygen being the oxygen donor. Monooxygenases catalyze the insertion of one oxygen atom into the substrate, while dioxygenases ensure the insertion of both atoms of dioxygen [46].

Examples of monooxygenases are methane monooxygenase, which catalyzes methane oxidation into methanol [16], and dopamine β-hydroxylase, whose vital function consists in noradrenaline synthesis by dopamine β-hydroxylation [47].

Methane monooxygenase was found in most of the known methanotrophic bacteria. According to their morphological and physiological properties, methanotrophic bacteria are divided into two enzyme systems, namely, the soluble system (sMMO) and the membrane-associated system (pMMO) [48]. The active site of sMMO, which has been properly investigated, contains two iron atoms. The membrane-associated methane monooxygenase system has been studied less comprehensively. It is hypothesized that pMMO has a type-2 copper site containing a single copper atom (Fig. 11) [49, 50].

The overall reaction catalyzed by a monooxygenase is

$$CH_4 + O_2 + NAD(P)H + H^+ \rightarrow CH_3OH + H_2O + NAD(P)^+.$$

The best known and most comprehensively studied enzyme among the copper-containing dioxygenases is quercetin 2,3-dioxygenase (Fig. 12).

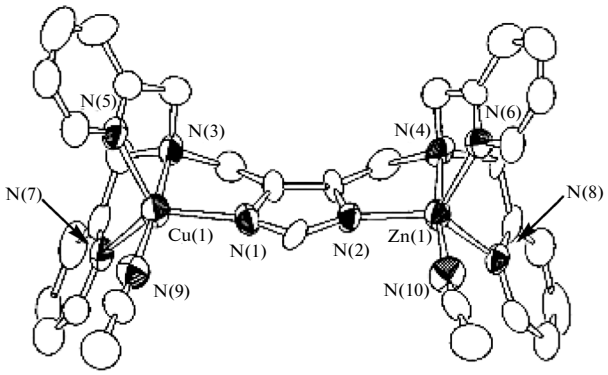

Fig. 16. Coordination compound $[CuZn(bdpi)(CH_3CN)_2](ClO_4)_3 \cdot 2CH_3CN$.

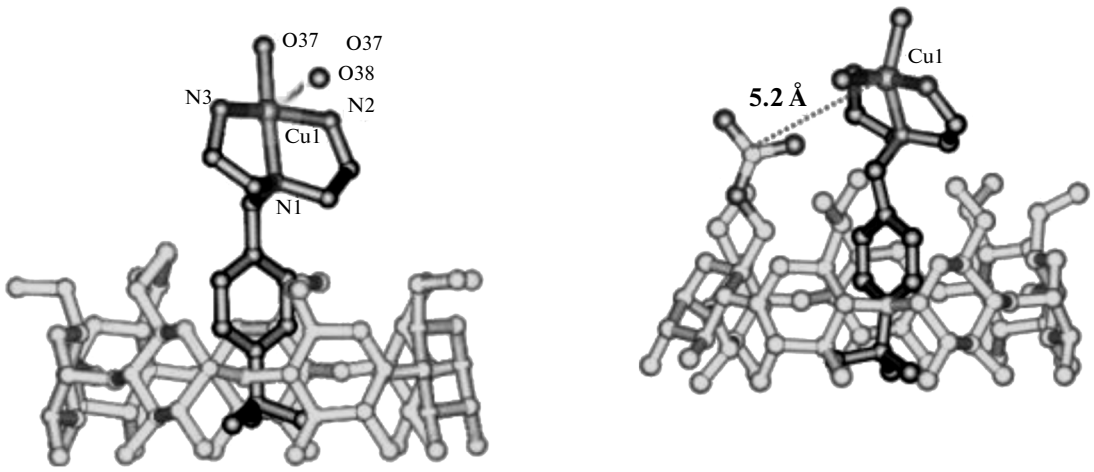

Fig. 17. Supramolecular modeling of copper complexes [37].

Quercetin 2,3-dioxygenase is the only iron-free dioxygenase whose crystal structure has been determined. The monomer of this enzyme contains a single copper atom, which is surrounded by three histidine residues and one water molecule that form a distorted tetragonal pyramid [52]. Steiner et al. [51] claim that there can also be a mixed trigonal bipyramidal and square pyramidal geometry of the ligand environment formed by three histidine residues (His66, His68, and His112), a solvent molecule (Wat_{tb}), and the side carboxylate chain Glu73.

Quercetin 2,3-dioxygenase catalyzes the cleavage of the *ortho*-heteroaromatic ring of flavonoids to yield depsides (esters of 4,6-dihydroxybenzoic acid) and carbon monoxide (Fig. 13) [53].

3.3. Dinuclear Enzyme Cu–Zn Superoxide Dismutase

Cu–Zn superoxide dismutase is a dimeric protein consisting of two subunits, one containing a copper(II) atom as the active site and the other containing a zinc(II) atom [54]. The copper atom is bonded to four histidine residues, and the zinc atom is bonded to three histidine residues and one aspartate residue (Fig. 14).

The dismutation (disproportionation) reaction catalyzed by superoxide dismutase is written in the following way [55]:

$$Cu^{2+} + O_2^- \rightarrow O_2 + Cu^+,$$

$$O_2^- + Cu^+ + 2H^+ \rightarrow H_2O_2 + Cu^{2+}.$$

Zinc is uninvolved in this reaction, but it is essential for the structure of the active site of the enzyme: the formation of the inter-subunit disulfide bond stabilizes the enzyme and plays an important role in the prevention of the aggregation of metal-deficient superoxide dismutase [56].

3.4. Examples of Low-Molecular-Weight Models of Type-2 Enzymes

It was demonstrated earlier that the presence of a copper ion is of crucial importance for the oxidation and reduction reactions catalyzed by Cu–Zn superoxide dismutase [57], but the role of the imidazole ring linking the copper and zinc atoms remains less clear [58].

Ohtsu et al. [58] synthesized a heteronuclear complex consisting of copper and zinc atoms and a 4,5-bis(di(2-pyridylmethyl)aminomethyl)imidazole ligand as a model of Cu–Zn superoxide dismutase (Figs. 15, 16).

This complex has the shape of a slightly distorted trigonal bipyramid.

The properties of the complex were studied by comparing them to the properties of the mononuclear and dinuclear coordination compounds between copper and this ligand. The cyclic voltammograms of the complex indicated much larger shifts to positive voltages (0.21 V and 0.19 V) than in the case of the analogous mononuclear and dinuclear copper–ligand complexes. By UV–vis spectroscopy and X-ray crystal-

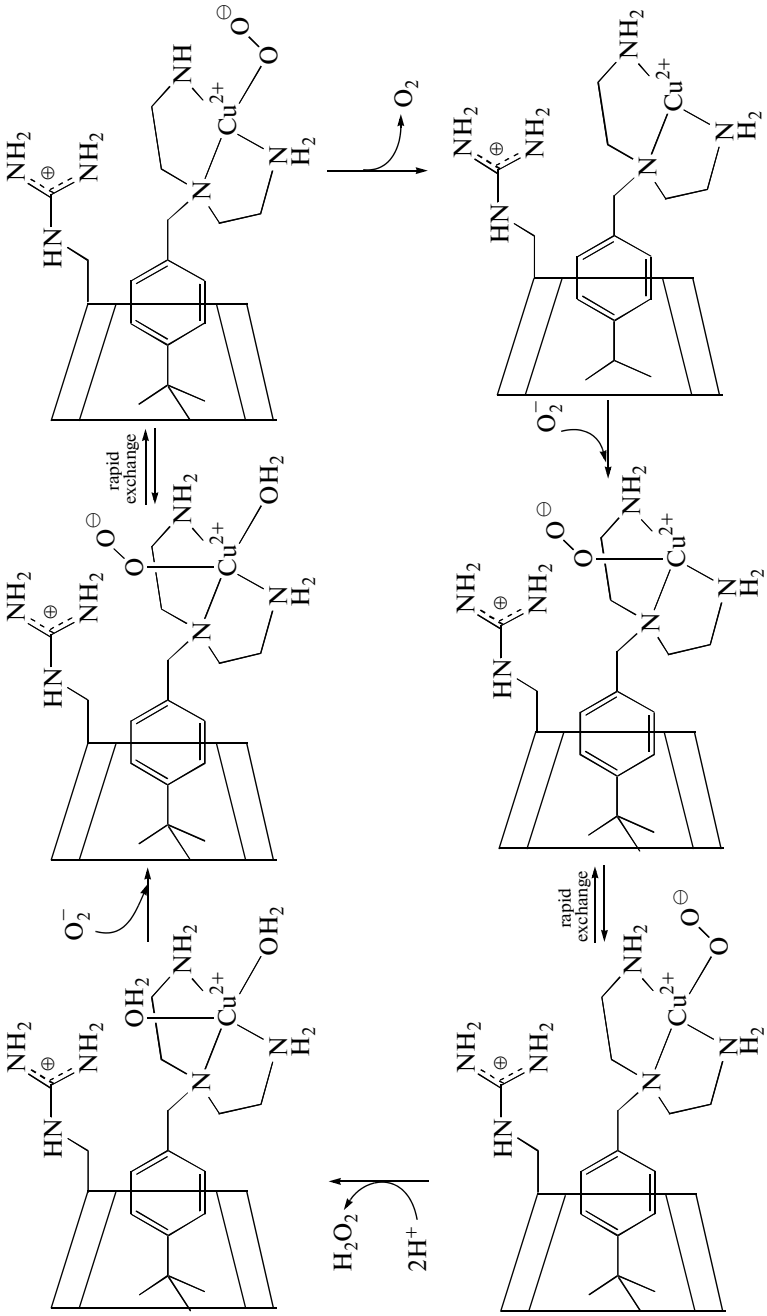

Fig. 18. Hypothetical mechanism of the dismutation of the supramolecular mimic containing a guanidyl cation.

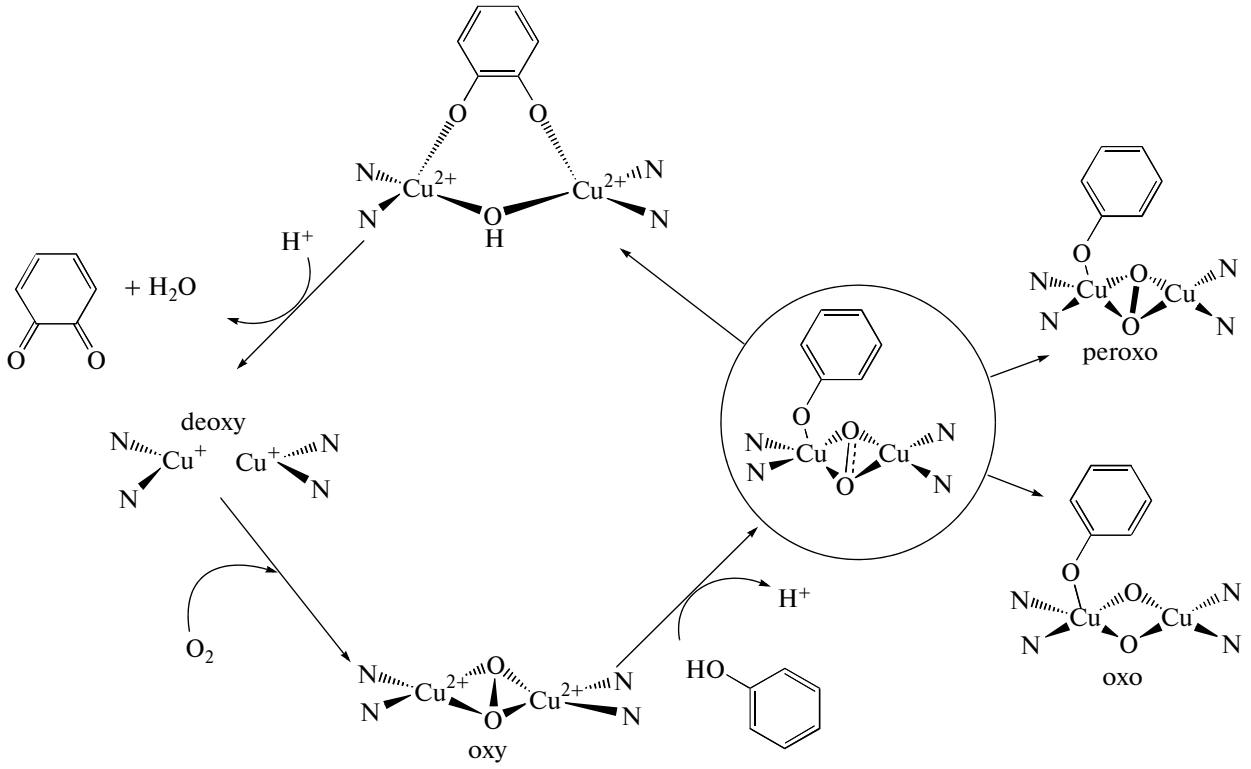

Fig. 19. Tyrosinase action mechanism [7, 62].

lography, it was found that the synthesized dinuclear copper–zinc complex is structurally similar to the active site of Cu–Zn superoxide dismutase [59].

The zinc ion, which can serve as a Lewis base, can also accelerate electron transfer from the Cu(I)–Zn(II) complex to the superoxide, since the superoxide is known to form a coordination compound with metal ions acting as Lewis acids to accelerate superoxide reduction through electron transfer [59, 60].

Interesting Cu–Zn superoxide dismutase mimics are supramolecular complexes containing a dinuclear copper(II) complex linked by an imidazole bridge with a fragment of β-cyclodextrin or a fragment of guanidyl-modified β-cyclodextrin [37]. Electronic absorption spectra of these complexes were recorded. The absorption maximum for both of them is between 619 and 622 nm. These values are close to the wavelength range observed for one of the Cu–Zn superoxide dismutase types (630–680 nm).

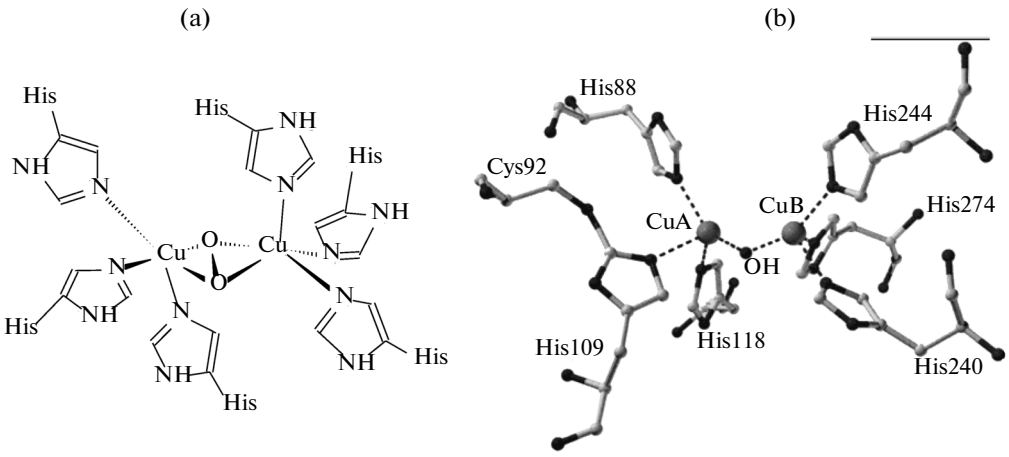

Fig. 20. Structure of the active site of hemocyanin: (a) oxy form and (b) reduced form [71].

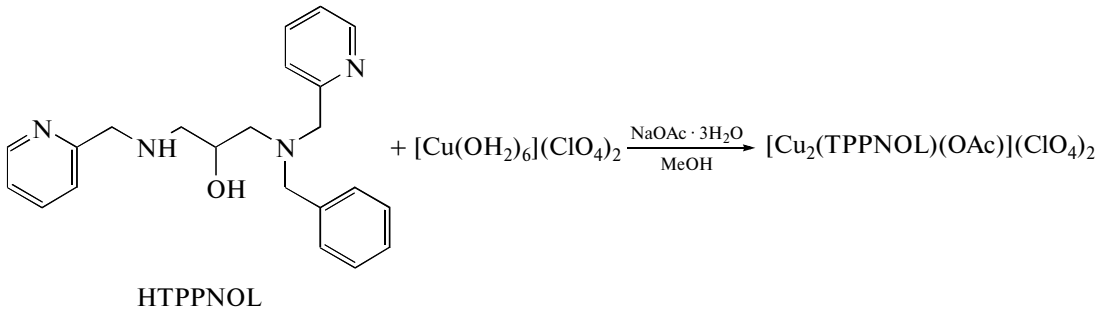

Fig. 21. Synthesis of the asymmetric dinuclear copper complex [73].

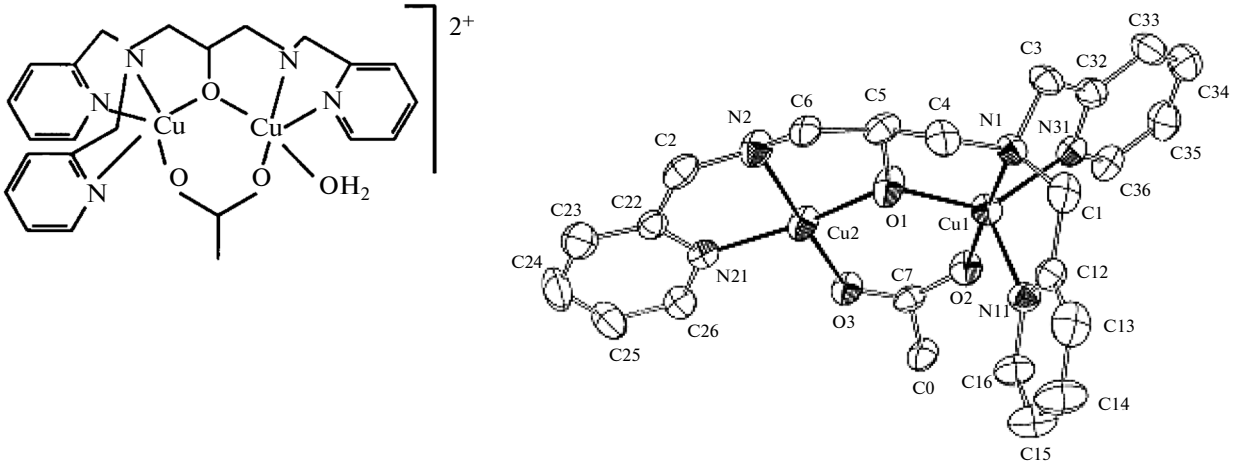

Fig. 22. Crystal structure of asymmetric dinuclear complex **1** simulating tyrosinase [73].

For the complexes presented in Fig. 17, studies of superoxide dismutase–imitating activity were conducted. These studies demonstrated that the IC_{50} value for the complex containing guanidyl-modified β-cyclodextrin is 40% larger than the IC_{50} value for the complex containing unmodified β-cyclodextrin.

Figure 18 presents a hypothetical mechanism of the dismutation of the complex whose structure includes guanidyl-modified β-cyclodextrin [37].

Under the action of the guanidyl cation, the superoxide anion approaches the copper(II) atom and binds directly to it. The superoxide anion bonded to the copper(II) atom can change rapidly between the

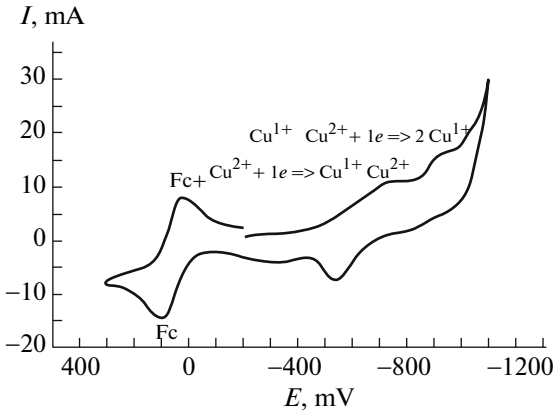

Fig. 23. Cyclic voltammogram of a solution of complex **1** in acetonitrile containing 1×10^{-3} M [TBA][PF_6] (platinum electrode, scan rate of 150 mV/s).

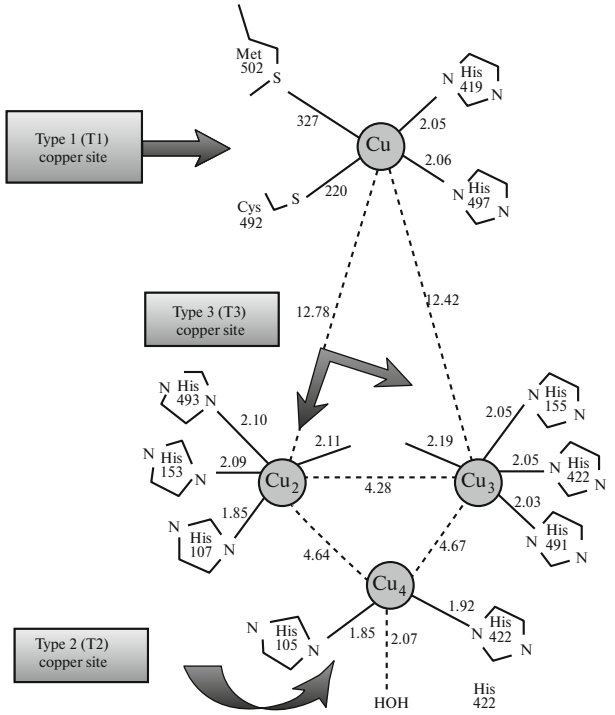

Fig. 24. Structure of laccase [74].

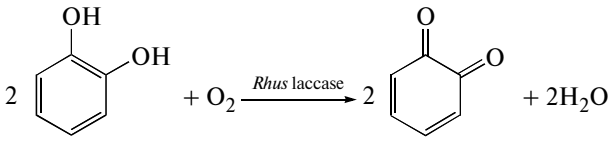

Fig. 25. Laccase-catalyzed oxidation reaction [81].

axial and basal positions of the distorted square pyramid in the molecule. This leads to a loss of an electron and to the formation of a free oxygen molecule, which then leaves the system. Thereafter, another superoxide anion binds to the copper(I) atom, and the molecule of the complex becomes capable of acting as an electron acceptor. Next, the molecule undergoes deprotonation, with the superoxide anion forming a neutral hydrogen peroxide molecule, which then leaves the system, thus completing the catalytic cycle.

4. TYPE-3 COPPER-CONTAINING ENZYMES

A distinguishing feature of type-3 copper-containing enzymes is that they have a pair of copper sites each coordinated by three histidine residues. The main functions of these enzymes are amino acid oxidation and oxygen transport. The geometry of a type-3 site is tetragonal. Type-3 enzymes do not contribute

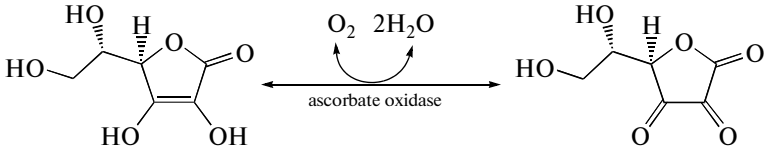

Fig. 26. Oxidation of L-ascorbic acid catalyzed by ascorbate oxidase.

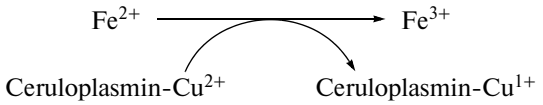

Fig. 27. Oxidation of the Fe^{2+} ion to Fe^{3+} catalyzed by ceruloplasmin.

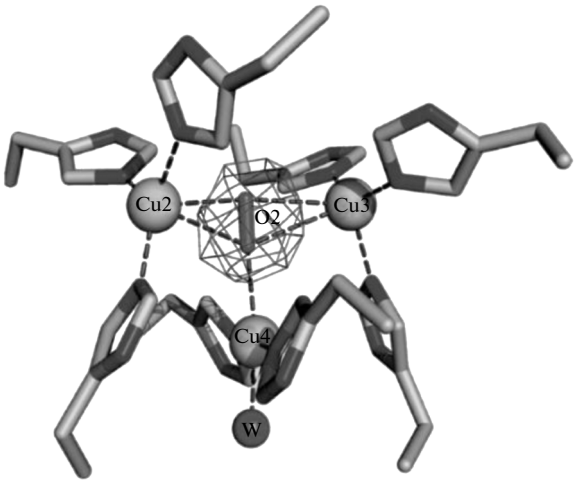

Fig. 28. Structure of the "trinuclear cluster" of ceruloplasmin.

to EPR spectra, because the interaction between two paramagnetic copper ions ($S = 1/2$) results in a diamagnetic state ($S = 0$) [61].

There are three type-3 enzymes: tyrosinase, catechol oxidase, and hemocyanin.

Tyrosinase is a hemocyanin-like dinuclear copper-containing protein. Tyrosinase activates oxygen and functions as a monooxygenase, hydroxylating phenols at their *ortho* position and then oxidizing the resulting catechol into *o*-quinone [7] (Scheme 2).

The main feature of tyrosinase is its capacity to catalyze the oxidation of the amino acid tyrosine (Fig. 19), which yields the black pigment melanin. Tyrosine is oxidized by this enzyme even when it is a component of a protein [7].

Since 1984, when the first model of tyrosinase was obtained, there have been numerous studies in this area, and tyrosinase mimics have been synthesized [62–69].

Hemocyanin, a respiratory pigment of the hemolymph of some invertebrates, has been attracting great attention from researchers since the late 1980s [70]. It contains two copper atoms that bind oxygen. Binding oxygen, the colorless site containing Cu(I) ions becomes blue owing to copper oxidation to Cu(II),

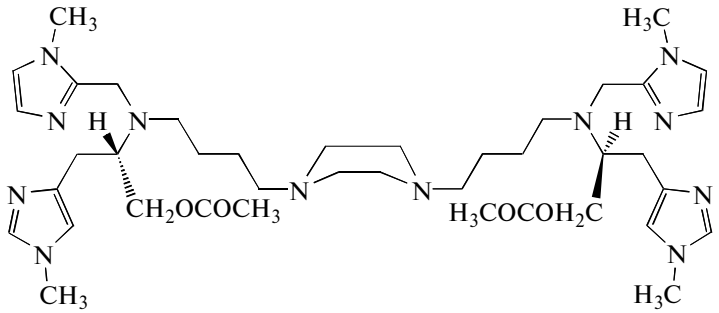

PHI

Fig. 29. Chiral ligand PHI that was used [89] in the synthesis of trinuclear cluster models.

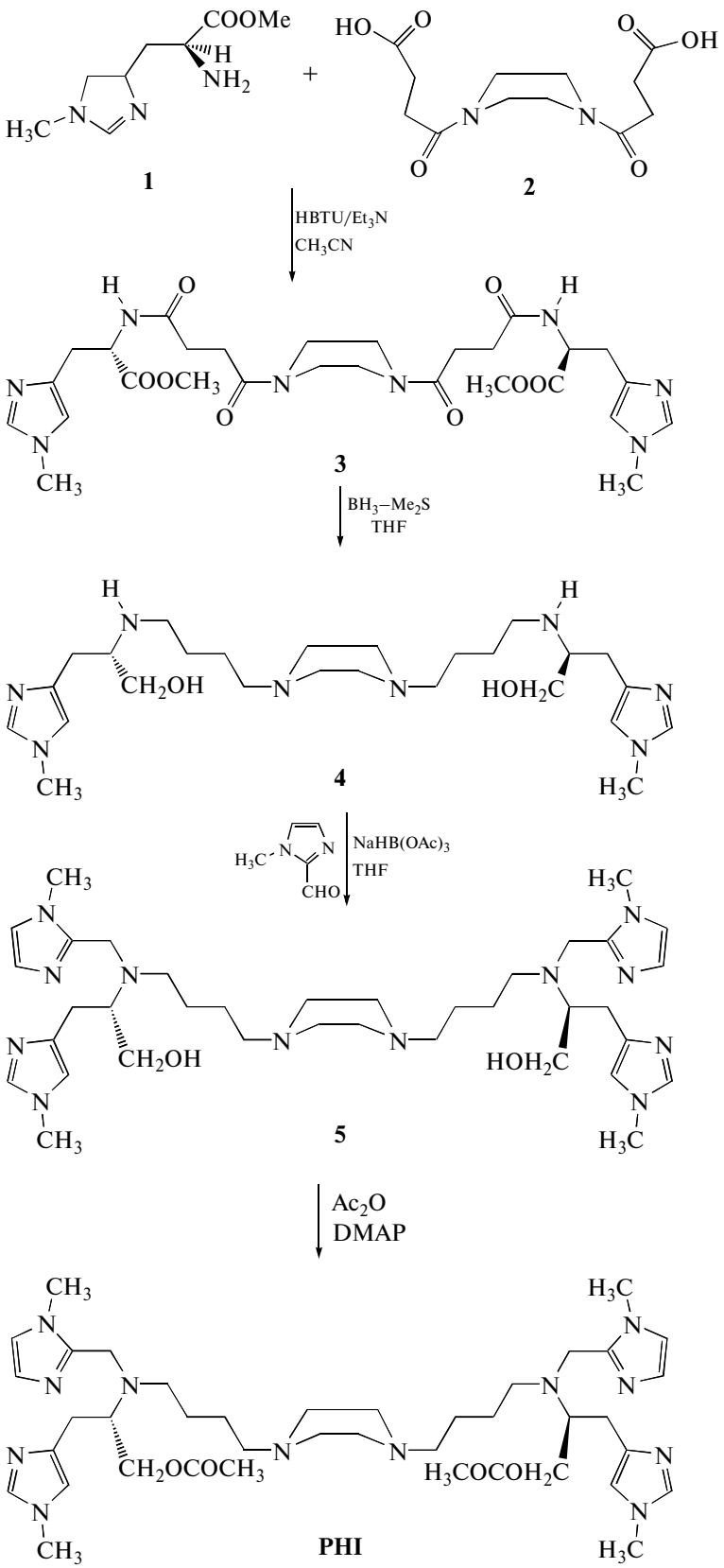

Fig. 30. Synthesis of the chiral ligand PHI.

(a)

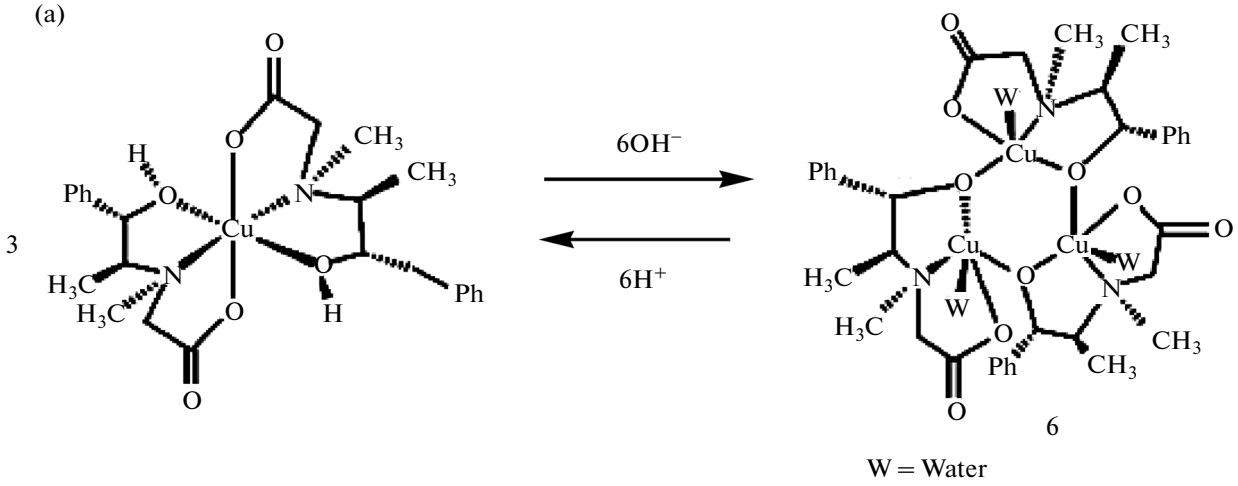

(b)

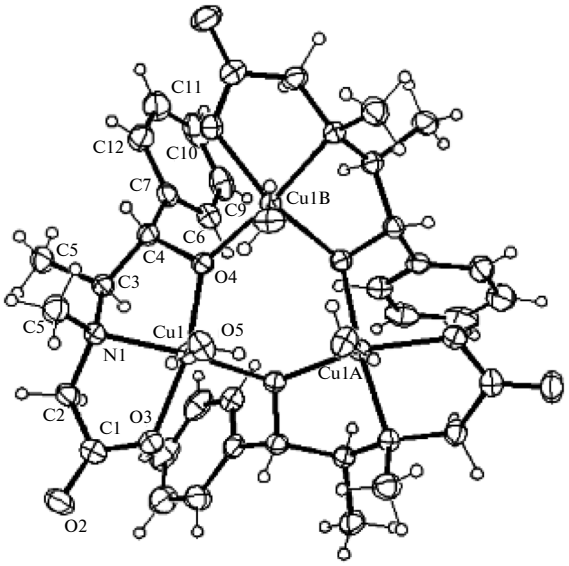

6

(c)

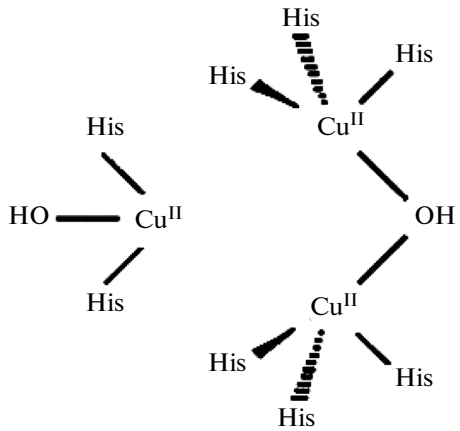

Fig. 31. (a) Reversible formation of complex **6** upon the addition of NaOH to the mononuclear complex; (b) crystal structure of complex **6**; (c) schematic representation of the mononuclear fragment of model compound **6** mimicking the trinuclear cluster of "blue" oxidases [90].

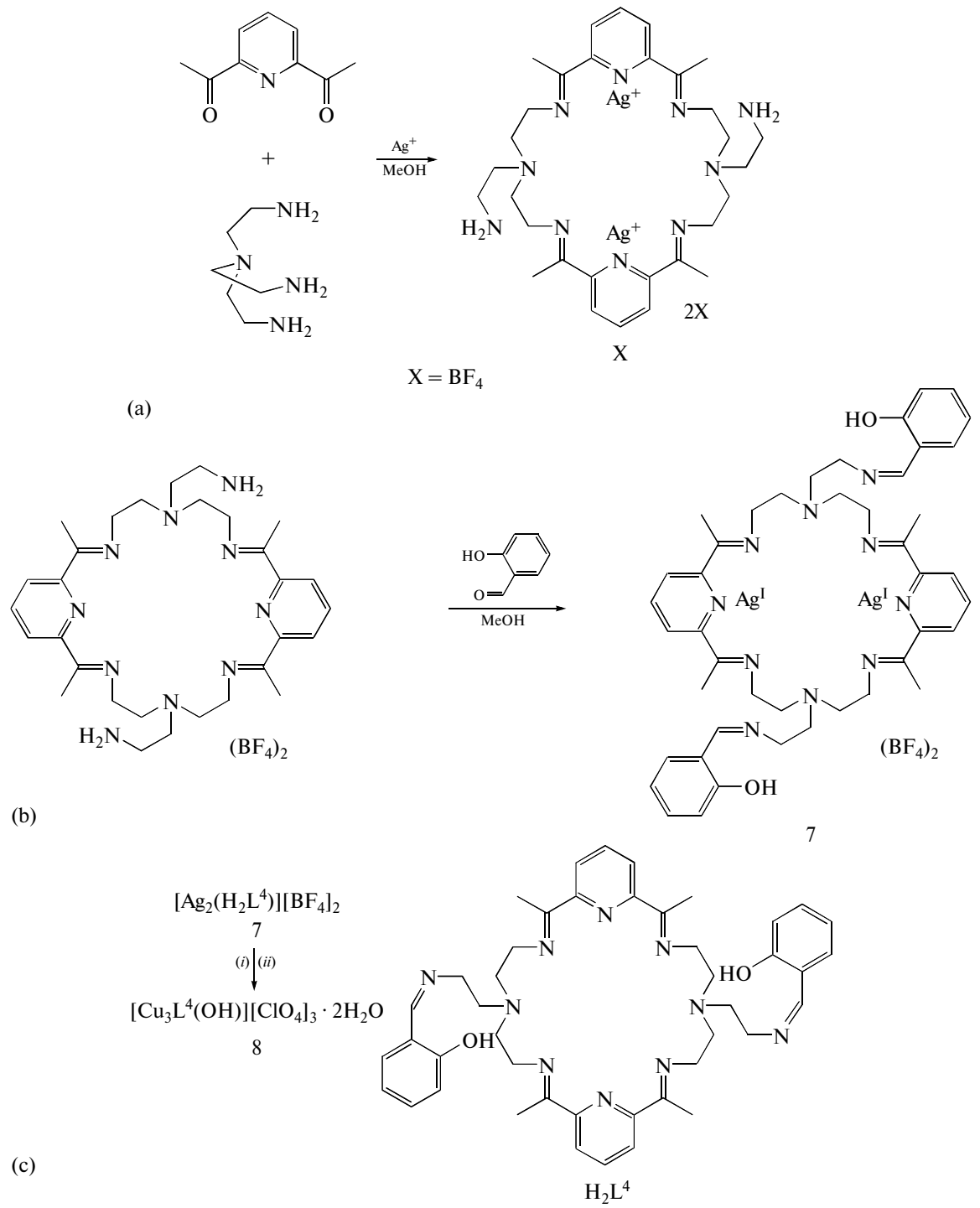

Fig. 32. (a) Synthesis of the macrocyclic silver complex; (b) functionalization of the macrocyclic silver complex; (c) transmetalation of the macrocyclic silver complex into the trinuclear copper(II) complex. (i) $Cu(MeCO_2)_2 \cdot 2H_2O$, $2Cu(BF_4)_2 \cdot 6H_2O$, MeOH–MeCN; (ii) $NaClO_4$, EtOH.

and this is the reason why the blood of most mollusks and some arthropod species is blue. This enzyme ensures oxygen transport in the blood, and its functions are similar to those of hemoglobin [7, 8, 19].

The active site of the protein contains two closely spaced copper cations ($d_{Cu-Cu} = 3.6$ Å), which reversibly bind an oxygen molecule into a complex. The copper cations are strongly fixed in the protein structure by six nitrogen atoms of the imidazole rings of histidine residues from two different chains [7].

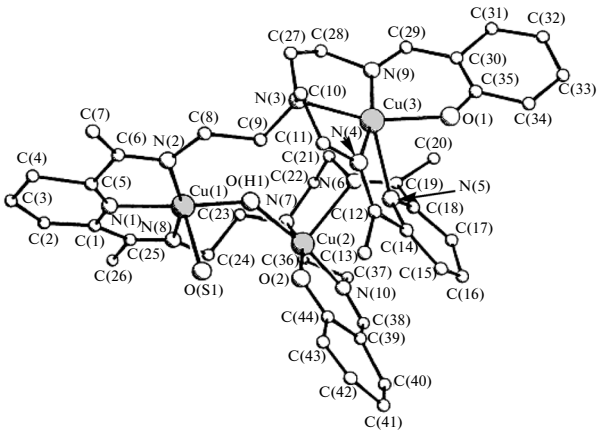

Fig. 33. Molecular structure of $[Cu_3L^4(OH)]^{3+}$ in complex **8**.

Low-molecular-weight analogs of the active site of this enzyme were synthesized, and the products of the interaction of these complexes with oxygen were obtained [8].

As for the general structure of this type of active site, the copper atoms in these dinuclear enzymes are linked together by a hydroxyl group and either copper atom is bonded to three nitrogen atoms of histidine. The oxy form additionally has bridging oxygen atoms (Fig. 20). Each copper atom is in a distorted tetrahedral ligand environment.

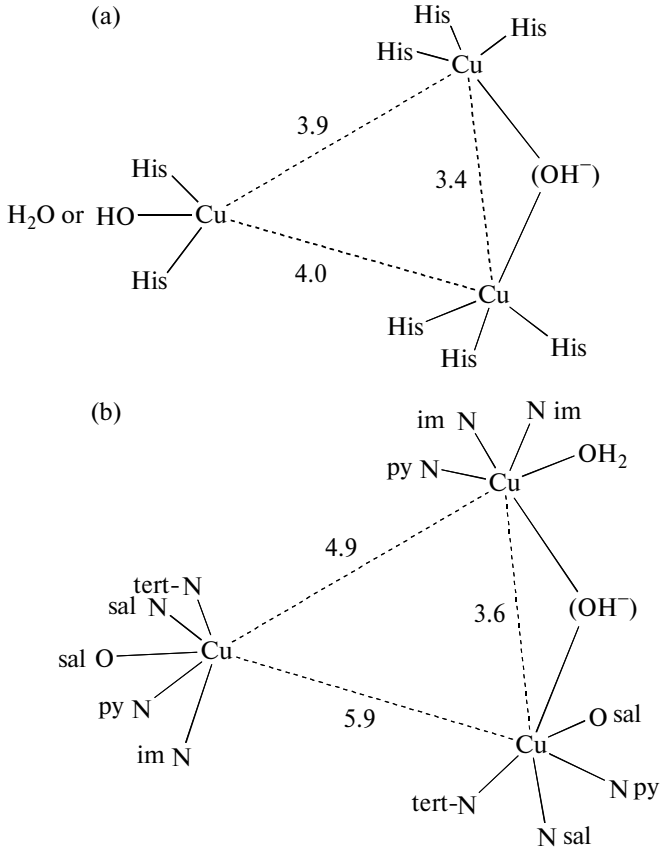

Fig. 34. (a) Structure of the trinuclear active site of ascorbate oxidase; (b) structure of the trinuclear site of coordination compound **8**. His = histidine residue, im N = imine nitrogen, py N = pyridine nitrogen, sal N = nitrogen of the salicylic moiety, sal O = oxygen of the salicylic moiety, and *tert*-N = tertiary amine nitrogen.

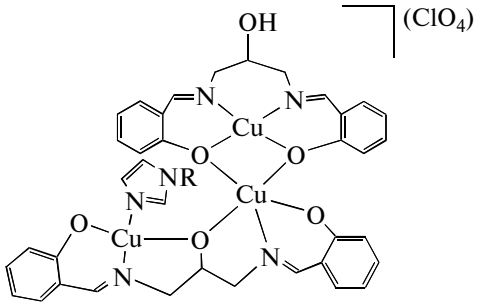

[R = H, 1; Me, 2]

Fig. 35. Structure of the dinuclear complex reported in [92].

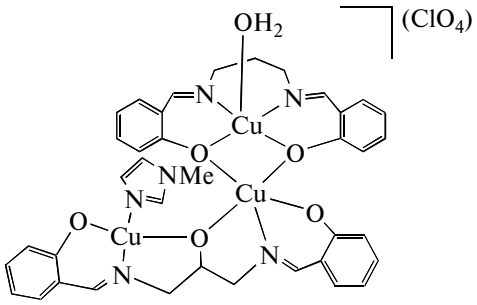

Fig. 36. Structure of the dinuclear complex reported in [93].

4.1. Examples of Low-Molecular-Weight Models of Type-3 Enzymes

In the dinuclear copper complexes that are low-molecular-weight models of hemocyanin and tyrosinase, either copper atom must be coordinated by three nitrogen atoms to repeat the coordination of the copper atoms in hemocyanin and tyrosinase [72].

There has been a report on the crystal structure and magnetic, redox, and spectral properties of the asymmetric dinuclear complex between copper(II) and *N,N,N′*-tris(2-pyridylmethyl)-1,3-diaminopropan-2-ol (HTPPNOL) [73] (Fig. 21).

This complex is a low-molecular-weight model of the active site of catechol oxidase and contains an acetate ion and a perchlorate ion, as was demonstrated by X-ray crystallography (Fig. 22).

One of the copper atoms in the complex is coordinated by five atoms (three nitrogen and two oxygen atoms) and is in a distorted trigonal bipyramidal ligand environment. The other copper atom is coordinated by two oxygen atoms and two oxygen atoms and is in a square-planar ligand environment. It was demonstrated that the complex oxidizes 3,5-di-*tert*-butylcatechol into the corresponding *ortho*-quinone.

In the investigation of amino acid oxidation catalyzed by type-3 enzymes, it is essential not only to synthesize and structurally characterize low-molecular-weight models and biomimetics of the enzymes but

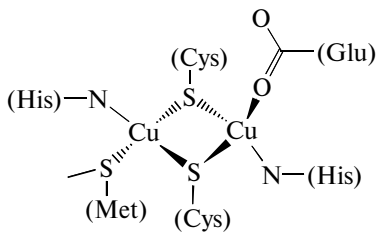

Fig. 37. Schematic representation of the Cu_A-type active site of cytochrome c oxidase.

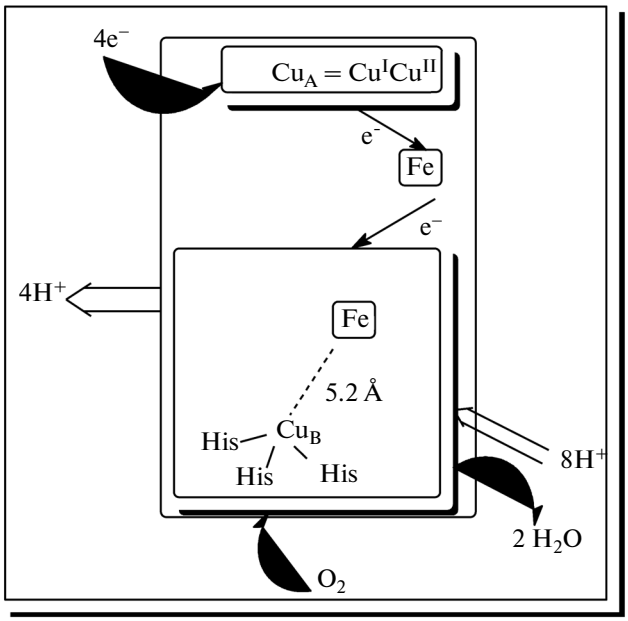

Fig. 38. Schematic representation of the active site of cytochrome c oxidase.

also to characterize them by electrochemical methods. For example, Fernandes et al. [73] reported a cyclic voltammogram of the synthesized complex in acetonitrile between −2.0 and 1.2 V (Fig. 23).

The cyclic voltammogram of the complex indicates two redox processes, one occurring at −0.38 V and the other at −0.56 V. The following irreversible process is assumed to take place:

$$2Cu^{2+} + 1\bar{e} \rightarrow Cu^{2+}Cu^{1+},$$

$$Cu^{2+}Cu^{1+} + 1\bar{e} \rightarrow 2Cu^{1+}.$$

5. TYPE-4 COPPER-CONTAINING ENZYMES (TYPE 2 + TYPE 3)

A type-4 active site generally combines types 2 and 3, forming a trinuclear cluster. The enzymes that additionally include a type-1 active site are assigned to "blue" oxidases. The type-2 copper atom is bonded to two histidine nitrogen atoms and a hydroxyl group and is separated by some distance from the dinuclear site (type 3), in which either copper atom is bonded to three histidine residues and is linked to the other copper atom by a hydroxyl group [19].

This type includes laccase (Fig. 24), ascorbate oxidase, and ceruloplasmin, whose function is catalysis of oxidation reactions.

Laccase is found in various microorganisms, plants, and fungi [75, 76]. Laccase contains three types of copper atoms. The type-1 copper site is responsible for the intense blue color of the enzyme and is characterized by an absorption band near 600 nm in the electronic absorption spectrum and shows itself in the EPR spectrum [77]. The presence of a type-2 copper site in laccase is indicated by EPR spectroscopy. This mononuclear site is colorless and does not show itself in the UV–vis spectral range. The type-3, dinuclear, diamagnetic copper site has two copper atoms that are undetectable by EPR spectroscopy; however, they give rise to a fairly diffuse shoulder near 330 nm in the absorption spectrum [77, 78]. The type-2 and type-

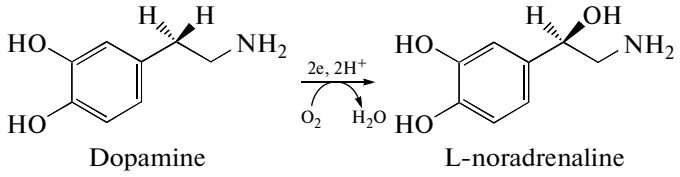

Fig. 39. Dopamine hydroxylation.

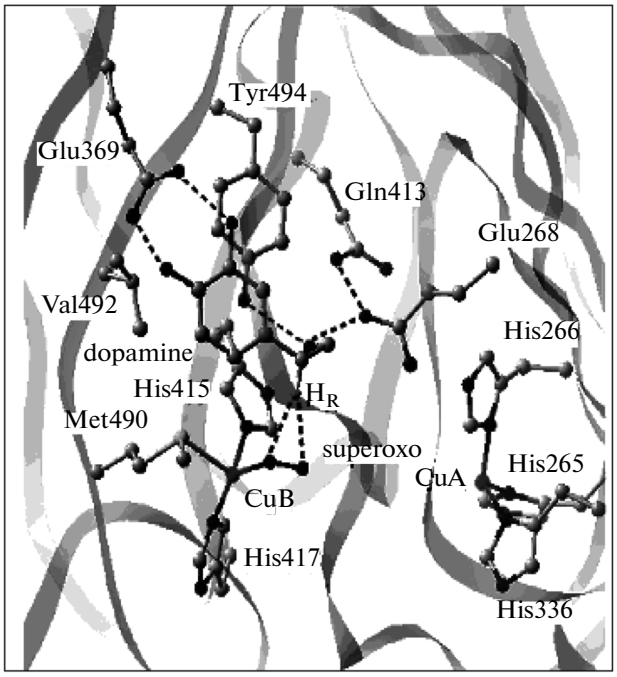

Fig. 40. Structure of the Cu_A- and Cu_B-type active sites of dopamine β–hydroxylase.

3 copper sites form a trinuclear cluster in which the type-2 copper atom is coordinated by two histidine residues and one water molecule. EPR data suggest that this fragment of the catalytic site is tetragonal or has the shape of a slightly distorted tetrahedron. The type-3 copper ions are surrounded by six histidine residues, and there is no bond between the type-2 and type-3 copper ions [74, 78, 79].

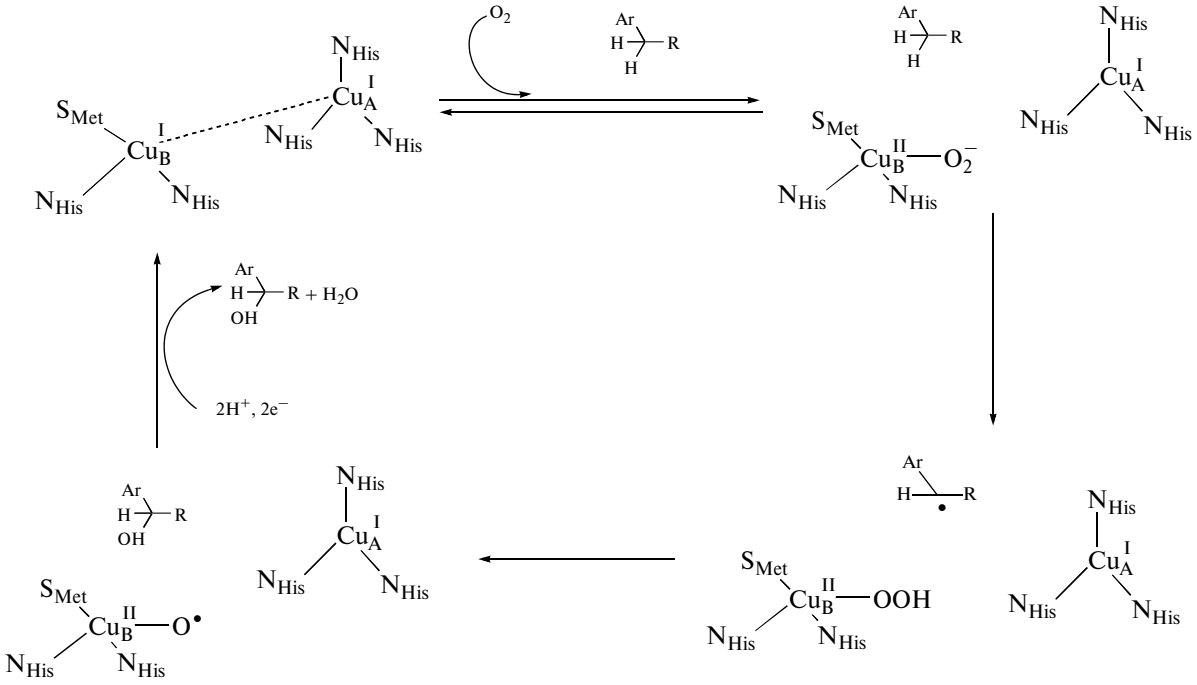

Fig. 41. Phenol hydroxylation mechanism [101].

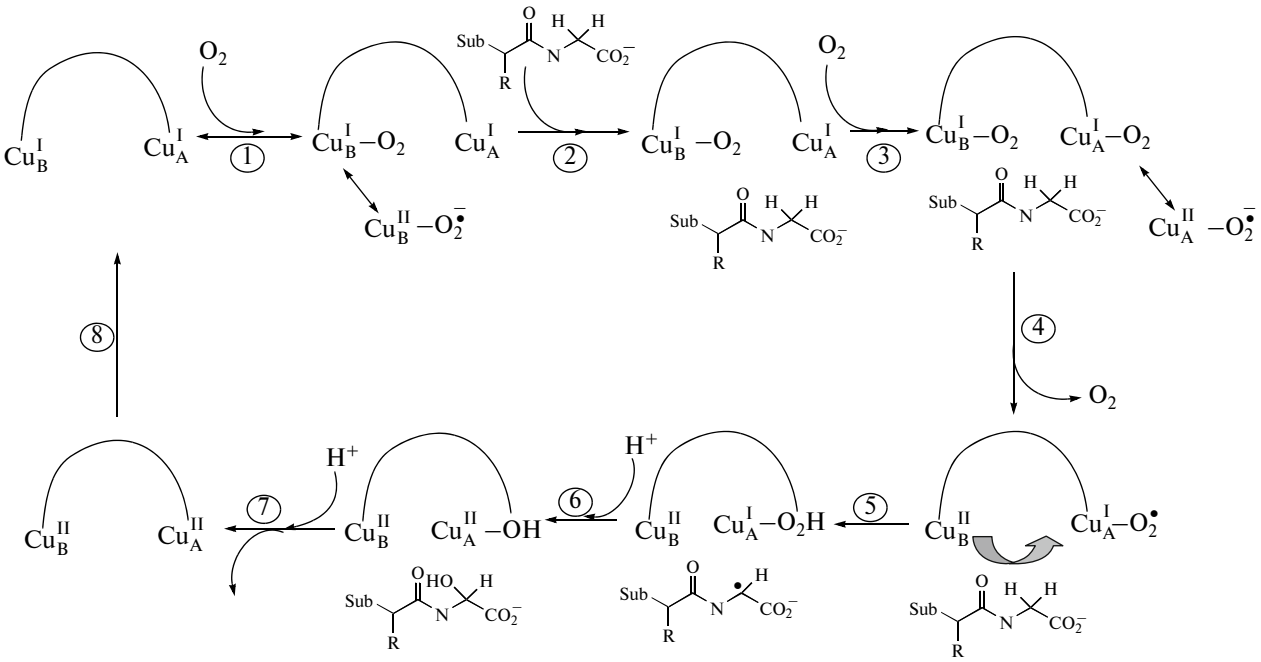

Fig. 42. Mechanism of the action of PAM on amides [100].

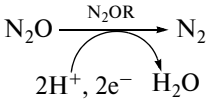

Fig. 43. Reduction of N_2O to N_2.

The main function of laccase is catalysis of oxidation reactions of organic substrates, such as phenols (Fig. 25) [80].

Ascorbate oxidase, a widespread enzyme, was found in many higher plants both in the soluble part of cells and in cell walls. The copper ion in the active site of this enzyme is in an asymmetric environment: the ligand in whose center the copper atom is located adopts a distorted configuration [82].

The presence of type-1 and type-2 copper ions in ascorbate oxidase is indicated by EPR spectroscopy, either type being characterized by its specific spectrum. The type-3 copper ions do not contribute to the EPR spectrum [83].

Ascorbate oxidase is a specific enzyme acting on ascorbic acid and its closest analogs [84]. The ascorbate oxidase–catalyzed oxidation of L-ascorbic acid into dehydro-L-ascorbic acid occurs via the reaction presented in Fig. 26.

The main function of ceruloplasmin, which is present in the human body and many mammals, is copper ion transport in the organism. Ceruloplasmin deficiency causes hepatocerebral dystrophy, which leads to poisoning of the organism by free copper ions [85]. In addition, ceruloplasmin catalyzes the oxidation of ascorbic acid, adrenalin, and dioxyphenylalanine [85]. It also oxidizes Fe^{2+} ions to Fe^{3+}, and the oxidized iron ions bind to the protein transferrin (Fig. 27) [86].

The ceruloplasmin structure resembles the laccase structure (Fig. 28). There are three types of copper ions in ceruloplasmin. The type-1 copper ion gives rise to an absorption peak at 610 nm. It interacts with two histidine nitrogens, with the SH group of cysteine, and with a methionine residue—the ligands forming its coordination sphere. The type-2 copper ion is characterized by an EPR spectrum typical of divalent copper and does not show itself in the optical spectrum. The two type-3 antiferromagnetic copper ions form a dinuclear copper complex that is characterized by an absorption maximum at 330 nm and is not detected by EPR spectroscopy [87]. As in the case of laccase, the type-2 copper ion and two type-3 copper ions form a “trinuclear cluster” [88].

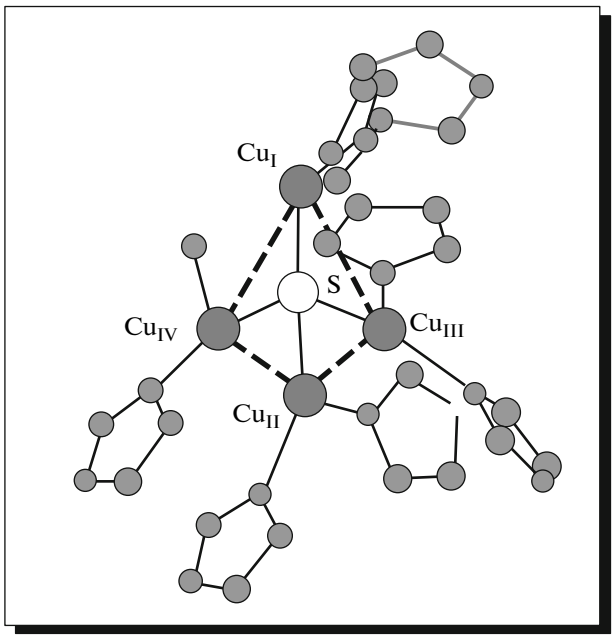

Fig. 44. Coordination of copper ions in the Cu_Z-type tetranuclear active site of N_2O reductase [5].

5.1. Examples of Low-Molecular-Weight Models of Type-4 Enzymes

There have been a considerable number of reports dealing with "blue" multicopper oxidases. However, some structural features of the "trinuclear clusters" that are the basic element of these copper-containing enzymes still remain unclear. This is the reason why it is essential to obtain synthetic analogs of laccase, ascorbate oxidase, and ceruloplasmin.

Santagostini et al. [89] reported the synthesis and a stereochemical study of dinuclear and trinuclear complexes simulating the copper clusters.

The chiral ligand PHI (Fig. 29), with two aminobis(imidazole) fragments, was included in the complex. A detailed scheme of PHI is presented in Fig. 30. The reaction between diacid **2** and *N*-methylhistidine methyl ether **1** afforded diamide **3**. The reduction of the carbonyl groups of **3** with $BH_3 \cdot Me_2S$ yielded compound **4**, which was then alkylated with 1-methyl-1*H*-imidazole-2-carbaldehyde and $NaBH(OAc)_3$ to obtain product **5**. Subsequent acylation in the presence of DMAP yielded the PHI ligand. The reaction between the target ligand PHI with a prescribed amount of copper perchlorate hexahydrate yielded the dinuclear complex $[Cu_2PHI][ClO_4]_4$ or the trinuclear complex $[Cu_3PHI][ClO_4]_6$.

UV–vis, CD, and EPR studies of these complexes demonstrated that the introduction of histidine residues into the ligand increases the value of these compounds as synthetic models of trinuclear copper clusters.

The following conditions should be met in the modeling of such a cluster:

The multidentate ligand must have eight donor nitrogen atoms (e.g., imidazole ring nitrogen atoms).

The ligand must be sufficiently flexible to allow geometric rearrangements.

The exogenous ligand must be capable of binding to metal sites [89].

Lopez-Sandoval et al. [90] demonstrated that variability of the stereochemistry of the molecule is among the important conditions for creating an appropriate model for the trinuclear cluster.

By examining the mononuclear moiety of one of the complexes synthesized by Lopez-Sandoval et al. [90], it was demonstrated that, for the *N*-[2-hydroxy-1(*R*)-methyl-2(*R*)-phenylethyl]-*N*-methylglycine ligand, which is the basic element of the mononuclear moiety, the energetically favorable form is the *threo* isomer (Fig. 31), in which the phenyl group and C–Ìå are in *trans* positions. It was also demonstrated that the *erythro* isomer of this compound cannot be isolated. It was concluded that the *threo*-to-*erythro* transition in the configuration of this ligand makes impossible the synthesis of models for the trinuclear clusters.

One of the earliest low-molecular-weight models of blue oxidases is the compound synthesized by Adams et al. [91]. By transmetalation of a macrocyclic disilver(I) complex (Fig. 32), they obtained the trinuclear macrocyclic complex $[Cu_3L_4(OH)][ClO_4]_3\,2H_2O$.

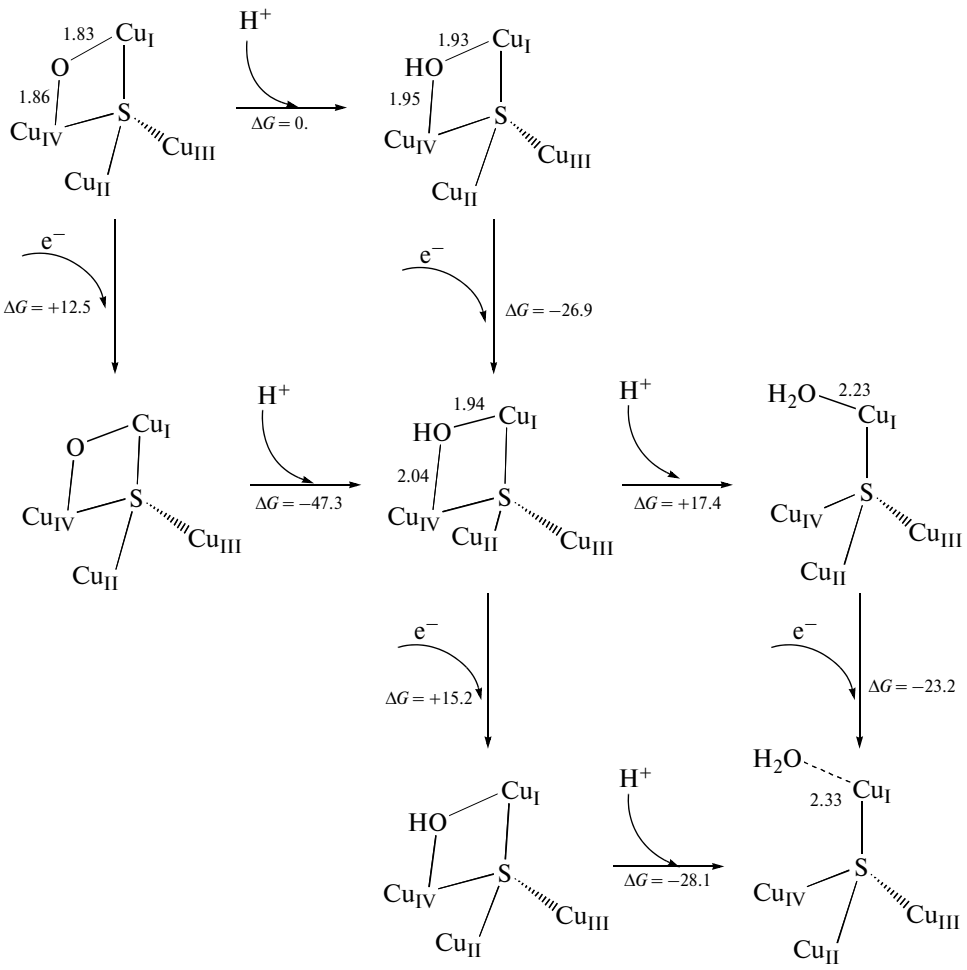

Fig. 45. Oxidized and reduced forms of the Cu_Z cluster in the catalytic cycle involving N_2O reductase. The imidazole moieties are omitted for the sake of simplicity. The interatomic distances are in angstroms. The Gibbs free energies (kcal/mol) were calculated for a temperature of 298 K [20].

An X-ray crystallographic study of the resulting complex showed that the trinuclear site is inside the macrocyclic ligand. The cluster consists of μ-hydroxy-bonded Cu(1) and Cu(2) atoms and a separate Cu(3) atom. The copper atoms in the complex can be considered to be in a distorted square-pyramidal environment.

The structure of the trinuclear complex (Fig. 33) is similar to the structure of the trinuclear cluster of ascorbate oxidase, as is demonstrated in Fig. 34 by comparing copper–copper bond lengths (Å).

An important point in the synthesis of analogs of trinuclear clusters is that the magnetic moment in the model should be close to the magnetic moment in the enzyme [92, 93].

Mukherjee et al. [92, 93] synthesized trinuclear copper(II) complexes by covalently bonding a monomeric fragment of a mimic with type-2 copper coordination to a dinuclear fragment with type-3 copper coordination (Fig. 35). The dinuclear fragment shows moderate antiferromagnetic interactions corresponding to the magnetic moment of the type-3 copper core in enzymes [92].

The complex reported in another work of those authors [93] simulates the active site of ascorbate oxidase and also has the magnetic properties of this structure (Fig. 36).

6. CU_A-TYPE COPPER-CONTAINING ENZYMES

This type of active site is also referred to as the mixed-valence site, since it contains two copper atoms each having a formal charge of +1.5 in the oxidized state. The ligand environment of either copper atom is a distorted tetrahedron. One of the copper atoms interacts, in the axial position, with the carbonyl oxygen atom of glutamine instead of interacting with sulfur (Fig. 37) [94].

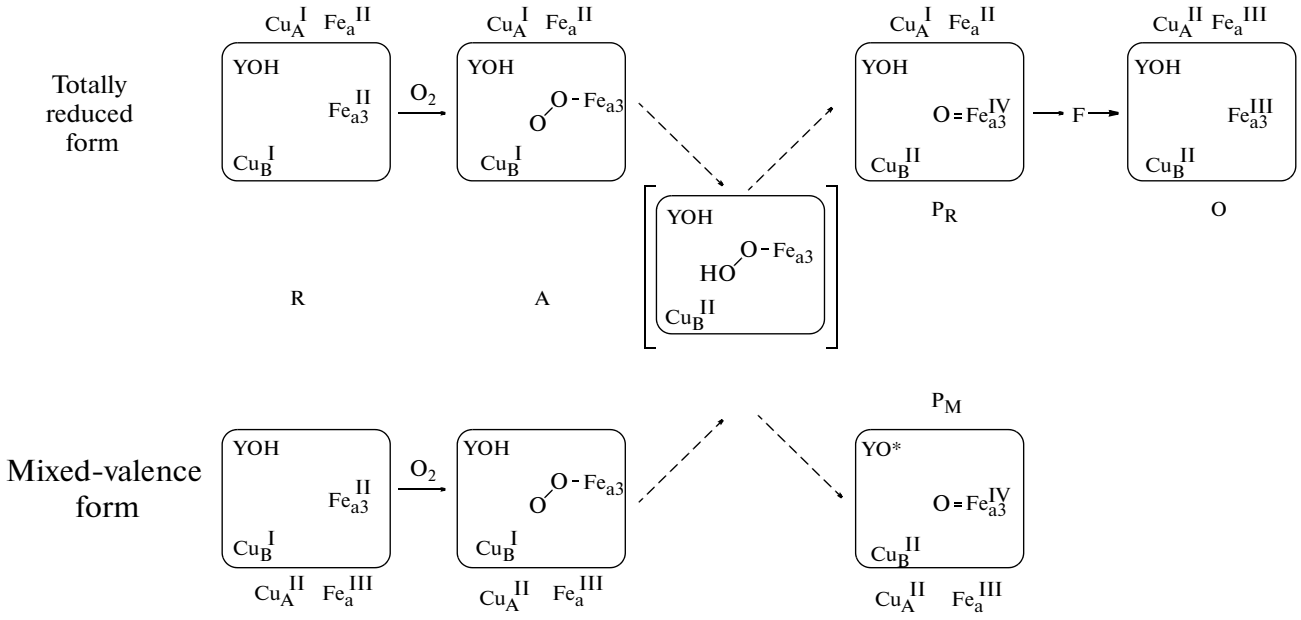

Fig. 46. Mechanism of oxygen reduction by the totally reduced and mixed-valence forms of cytochrome c oxidase (YOH = tyrosine residue) [112].

The electronic spectra of Cu_A-type enzymes in the UV–vis range show three absorption bands at 480, 530, and 800 nm. The bridging sulfur atoms of cysteine play a significant role in the structural study of enzymes and largely determine their redox, spectral, and catalytic properties [94, 95]. In addition, the EPR spectra of cytochrome c oxidase and nitrite reductase demonstrated that the $\tilde{N}u_A$ site is similar in properties to the dinuclear copper site of nitrite reductase and has the mixed-valence configuration [Ñu(1.5)...(Cu(1.5)] [96].

The Cu_A-type site occurs in cytochrome c oxidase. This enzyme is an important element of cellular respiration (oxygen transport through the cell membrane). Its active site consists of two types of sites, namely, a Cu_A site, which is responsible for electron transfer, and a Cu_B site, which binds oxygen and converts it into water (Fig. 38) [97, 98].

It is clear from the above scheme that the chemical equation of the overall process is $O_2 + 4e^- + 4H^+ 2H_2O$ [98].

7. CU_B-TYPE COPPER-CONTAINING ENZYMES

The function of the Cu_B (or Cu_M) site in, e.g., dopamine β-hydroxylase [99] is binding to, and hydroxylation of, the substrate; in peptidylglycine α-amidating monooxygenase, (PAM), this site is responsible for electron transfer [100]. This type of site is most comprehensively studied in cytochrome c oxidase, whose main biological role is four-electron water reduction to water. The copper atom in this type of site is in a trigonal pyramidal ligand environment and is bonded to three nitrogen atoms of histidine.

Dopamine β-hydroxylase catalyzes dopamine hydroxylation into the neurotransmitter noradrenaline (Fig. 39) [99].

This enzyme contains two types of active sites—Cu_A and Cu_B. Two metal atoms from these sites are separated by a distance of about 11 Å [101], and this was confirmed by EPR data indicating no spin–spin coupling in the system (Fig. 40). It was also demonstrated by EPR spectroscopy that the copper atoms are in the oxidized state and are elements of the following structures: $Cu_A(His)_3(H_2O)$ and $Cu_B(His)_2X(H_2O)$, where Õ is the histidine residue or an oxygen donor ligand [102].

As was mentioned above, the main role in the hydroxylation mechanism is played by the $Cu_{\tilde{A}}$ site; for this reason, in the scheme presented in Fig. 41, we consider only one copper atom of the $Cu_{\tilde{A}}$-type site [101].

PAM is a bifunctional enzyme capable of catalyzing the conversion of peptides having a glycine residue at the C-terminus (including their native L-forms) into the corresponding peptidyl amides [7]. Like

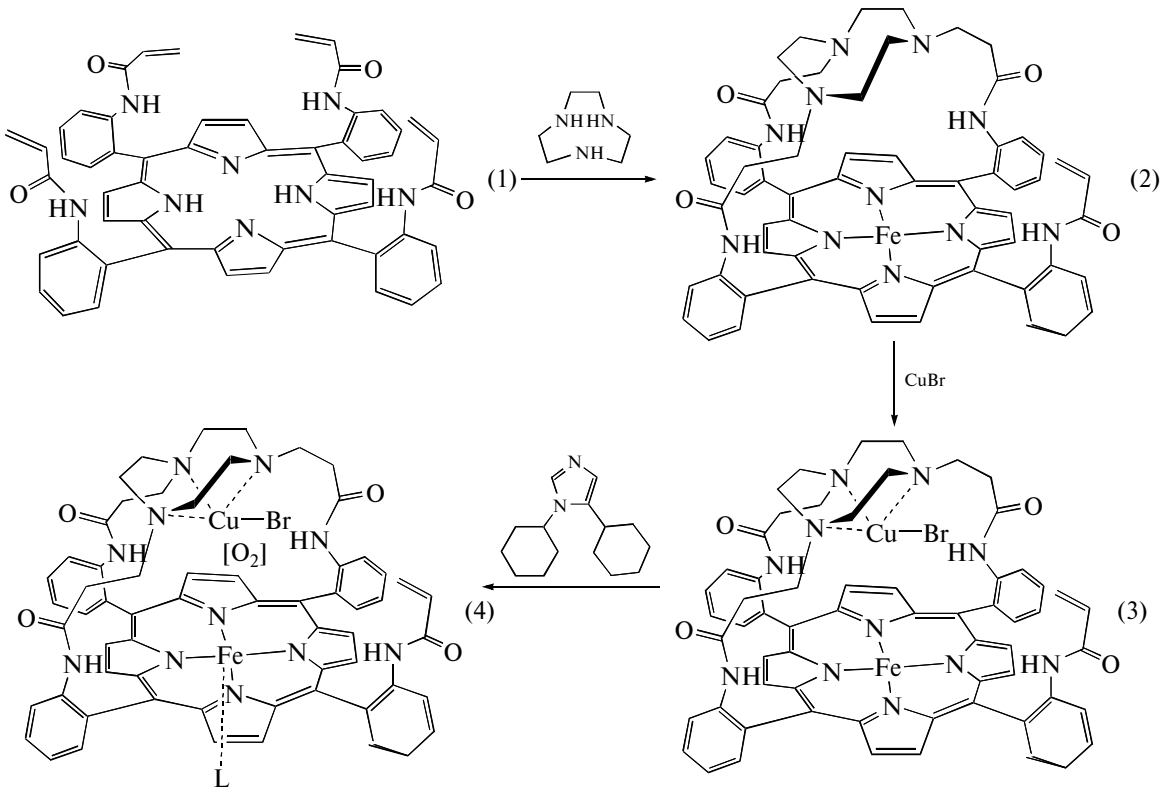

Fig. 47. Synthesis of cytochrome c oxidase biomimetic **4** [114].

dopamine β-hydroxylase, PAM has two types of active sites, namely, Cu_A and Cu_B [100, 101], but in PAM, the Cu_A site is responsible for oxygen–substrate binding and for substrate activation, while the Cu_B site is responsible only for electron transfer (Fig. 42).

This oxidative cleavage is the basic process in the bioactivation of many protein hormones and neuropeptides. A number of chemical models of PAM were studied earlier [100], but the C–N bond cleavage mechanism has not been completely elucidated, even though there are crystallographic data partly explaining the above scheme [7].

8. CU_Z-TYPE COPPER-CONTAINING ENZYMES

The Cu_Z-type site contains four copper atoms linked by a μ_4-sulfide bridge to a sulfur atom and has the shape of a distorted tetrahedron. Altogether, the four copper atoms are bonded to seven nitrogen atoms: three of them are bonded to two nitrogen atoms each, and the fourth is bonded to only one nitrogen atom and to an oxygen atom [103–105].

The only representative of this enzyme type is N_2O reductase (N_2OR). This enzyme is responsible for N_2O reduction to N_2 at the last stage of the nitrogen cycle in nature [103, 106]. The general scheme of nitrous oxide reduction is presented in Fig. 43.

This enzyme contains two types of active sites, namely, Cu_A, which is responsible for electron transfer, and the catalytic site Cu_Z [103, 104, 106]. The structure of the Cu_Z-type site is shown in Fig. 44.

Although the N_2O molecule is kinetically inert ($E_A \sim 59$ kcal/mol), the Cu_Z-type site lowers the energy barrier from $\Delta G = 18$ kcal/mol to $\Delta G = 9–13$ kcal/mol through noncovalent interactions (hydrogen bonding) [107] and breaks the N–O bond by increasing the electron density through Cu(I)–N_2O interaction [108, 109].

The hypothetical mechanism of energy barrier lowering in the Cu_Z cluster for subsequent N–O bond breaking is presented in Fig. 45 [107].

Proton transfer in this mechanism is directly combined with the N–O bond breaking stage, and the activation barrier here can be reduced to zero. Thus, at low pH (4–8), the rate-limiting step in the cata-

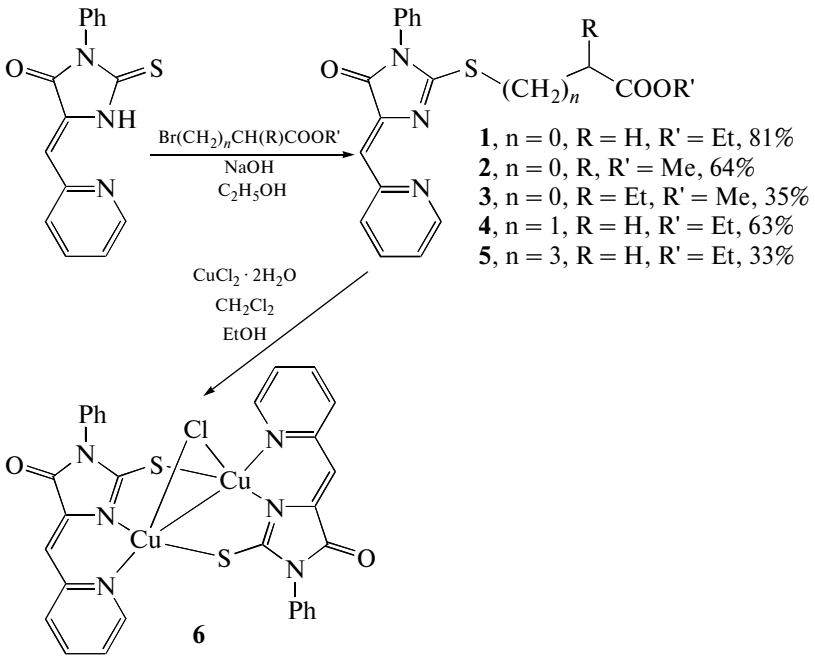

Fig. 48. Synthesis of the biomimetic based on a derivative of 2-thioxo-3-phenyl-5-(pyridin-2-ylmethylene)-3,5-dihydro-4*H*-imidazol-4-one [116].

lytic cycle of N_2O reductase is electron transfer from the reductant to the Cu_Z cluster rather than N–O bond cleavage.

Oganesyan et al. [110] characterized N_2O reductase by EPR spectroscopy and demonstrated that the tetranuclear moiety of the enzyme is a delocalized mixed-valence system.

8.1. Examples of Low-Molecular-Weight Models of Cytochrome c Oxidase and N_2O Reductase

At present, synthetic analogs of cytochrome c oxidase, dopamine-β-hydroxylase, and N_2O reductase are of particular interest, since they are necessary objects in the investigation of the mechanism of action of these enzymes.

Examples of cytochrome c oxidase models. In recent years, there have been an increasing number of publications dealing with development and study of such compounds. However, none of the bioinorganic complexes reproduces the heme–superoxide heteronuclear structure characteristic of cytochrome c oxidase [111]. The metal site of the enzyme is a combination of an iron atom (component of myoglobin) and a tris-histidine-coordinated copper atom [112]. The reduction of the oxygen molecule to the water molecule and rapid electron transfer from cytochrome c to the heme active site $\dot{a}_3/Cu_B$ are due to the presence of a homodinuclear copper site and a mononuclear heme *a* in the enzyme. The general scheme of the reduction process is presented in Fig. 46.

The nature of intermediates in the reduction of oxygen by cytochrome c oxidase depends on their redox state. While the heme/Cu site must be in the "iron–copper" state for binding an oxygen molecule, the other cofactors may be in the totally oxidized state (examples are mixed-valence forms of the enzyme) [113].

The synthetic enzyme analog considered by Collman et al. [114] is obtained by the series of reactions presented in Fig. 47. The metalation of Michael acceptor **1** with iron followed by the addition of 1,4,7-triazacyclononane yields product **2,** which is then metalated with CuBr to obtain the cytochrome c oxidase model **3.** Like all related native enzymes, compound **3** contains a porphyrin iron atom located in the immediate vicinity of a copper(I) atom. The addition of excess 1,5-dicyclohexylimidazole shifts the central iron atom to an axial position, as in the corresponding enzyme, and yields compound **4** [111, 114].

Examples of N_2O reductase models. The main purpose of development of small synthetic analogs of this enzyme is to study its geometry, electronic structure, and protein matrix.

The following two ways of classifications of N_2O-reductase models were suggested:

Classification according to the type of reaction used to synthesize the complex [108]:
reactions of Cu(I) complexes with elemental sulfur;
reactions of Cu(II) complexes with sulfur-containing compounds.
Classification according to the type of complex [115]:
dinuclear complexes;
trinuclear complexes;
polynuclear complexes.

Synthetic N_2O reductase models can also be divided into Cu_Z model clusters and mixed-valence complexes mimicking the Cu_A-type site.

There has been a report [116] on the synthesis and physicochemical study of a new mixed-valence copper complex, namely, a derivative of 2-thioxo-3-phenyl-5-(pyridin-2-ylmethylene)-3,5-dihydro-4*H*-imidazol-4-one (compound **6** in Fig. 48), which is a promising biomimetic of the N_2O reductase active site.

It was demonstrated that, in this complex, the copper–copper distance is 2.562 Å, which is close to the Cu_I–Cu_{IV} distance in the active site of N_2O reductase. The fact that the copper atoms in the complex have geometrically identical surroundings suggests that the complex is in a delocalized mixed-valence form structurally similar to the Cu_A-type site. In addition, it was demonstrated that the synthesized coordination compound is catalytically active: it catalyzed nitrous oxide reduction with PPh_3.

York et al. [115] systematized low-molecular-weight structures that can display N_2O reductase activity and can potentially reduce N_2O to N_2. Bimolecular, trimolecular, and macromolecular models of the Cu_Z site were developed, and it was demonstrated that the nature and properties of these clusters depend considerably on the nitrogen atoms of the ligand, on the source of sulfur atoms, on the copper salt type, and on the reaction conditions [117–119].

REFERENCES

1. Chistyakov, Yu.V., *Osnovy bioneorganicheskoi khimii* (Fundamentals of Bioinorganic Chemistry), Moscow: Khimiya. KolosS, 2007.
2. Klinman, J.P., *Chem. Rev.*, 1996, vol. 96, no. 7, p. 2541.
3. Solomon, E.I., Sundaram, U.M., and Machonkin, T.E., *Chem. Rev.*, 1996, vol. 96, no. 7, p. 2563.
4. Holmberg, C.G., and Laurell, C.-B., *Acta Chem. Scand. (1947–1973)*, 1948, vol. 2, p. 550.
5. Solomon, E.I., Sarangi, R., Woertink, J.S., Augustine, A.J., Yoon, J., and Ghosh, S., *Acc. Chem. Res.*, 2007, vol. 40, no. 7, p. 581.
6. Murphy, M.E.P., *Cell. Mol. Life Sci.*, 2007, vol. 64, no. 22, p. 2887.
7. Gamez, P., Aubel, P.G., Driessen, W.L., and Reedijk, J., *Chem. Soc. Rev.*, 2001, vol. 30, no. 6, p. 376.
8. Mirica, L.M., Ottenwaelder, X., and Stack, T.D.P., *Chem. Rev.*, 2004, vol. 104, no. 2, p. 1013.
9. Chaudhari, A., Mahfouz, M., Fialho, A.M., Yamada, T., Granja, A.T., Zhu, Y., Hashimoto, W., Schlarb-Ridley, B., Cho, W., Gupta, T.K.D., and Chakrabarty, A.M., *Biochemistry*, 2007, vol. 46, no. 7, p. 1799.
10. Marshall, N.M., Garner, D.K., Wilson, T.D., Gao, Y.-G., Robinson, H., Nilges, M.J., and Lu, Y., *Nature*, 2009, vol. 462, no. 7269, p. 113.
11. Tisato, F., Marzano, C., Porchia, M., Pellei, M., and Santini, C., *Med. Res. Rev.*, 2010, vol. 30, no. 4, p. 708.
12. Duncan, C., and White, A.R., *Metallomics*, 2012, vol. 4, no. 2, p. 127.
13. Iakovidis, I., Delimaris, I., and Piperakis, S.M., *Mol. Biol. Int.*, 2011, 594529.
14. Choi, M., and Davidson, V.L., *Metallomics*, 2011, vol. 3, no. 2, p. 140.
15. Kim, E., Helton, M.E., Wasser, I.M., Karlin, K.D., Lu, S., Huang, H.-W., Moenne-Loccoz, P., Incarvito, C.D., Rheingold, A.L., Honecker, M., Kaderli, S., and Zuberbuhler, A.D., *Proc. Natl. Acad. Sci.*, 2003, vol. 100, no. 7, p. 3623.
16. Lieberman, R.L., and Rosenzweig, A.C., *Dalton Transþ*, 2005, no. 21, p. 3390.
17. Sosna, M., Chretien, J.-M., Kilburn, J.D., and Bartlett, P.N., *Phys. Chem. Chem. Phys.*, 2010, vol. 12, no. 34, p. 10018.
18. Pomowski, A., Zumft, W.G., Kroneck, P.M.H., and Einsle, O., *Nature*, 2011, vol. 477, no. 7363, p. 234.
19. Koval, I.A., Gamez, P., Belle, C., Selmeczi, K., and Reedijk, J., *Chem. Soc. Rev.*, 2006, vol. 35, no. 9, p. 814.
20. Messerschmidt, A., *Ascorbate Oxidase*, New York: Springer, 2013.
21. Valentine, J.S., and Gralla, E.B., *Copper-Containing Molecules*, Elsevier, 2002.
22. Canters, G.W., and Gilardi, G., *FEBS Lett.*, 1993, vol. 325, nos. 1–2, p. 39.
23. Remenyi, C., Reviakine, R., and Kaupp, M., *J. Phys. Chem. B*, 2007, vol. 111, no. 28, p. 8290.

24. Baniulis, D., Yamashita, E., Zhang, H., Hasan, S.S., and Cramer, W.A., *Photochem. Photobiol.*, 2008, vol. 84, no. 6, p. 1349.
25. Kabashnikova, L. *Fotosinteticheskii apparat i potentsial produktivnosti khlebnykh zlakov* (Photosynthetic Apparatus and Productivity Potential of Cereals), Minsk: Belarus. navuka, 2011.
26. Varfolomeev, S.D. and Zaitsev, S.V., *Kineticheskie metody v biokhimicheskikh issledovaniyakh* (Kinetic Methods in Biochemical Studies), Moscow: Mosk. Gos. Univ., 1982.
27. Jones, T.E., Rorabacher, D.B., and Ochrymowycz, L.A., *J. Am. Chem. Soc.*, 1975, vol. 97, no. 26, p. 7485.
28. Holland, P.L., and Tolman, W.B., *J. Am. Chem. Soc.*, 2000, vol. 122, no. 26, p. 6331.
29. Romero, A., Hoitink, C.W.G., Nar, H., Huber, R., Messerschmidt, A., and Canters, G.W., *J. Mol. Biol.*, 1993, vol. 229, no. 4, p. 1007.
30. Karlsson, B.G., Tsai, L.-C., Nar, H., Sanders-Loehr, J., Bonander, N., Langer, V., and Sjolin, L., *Biochemistry*, 1997, vol. 36, no. 14, p. 4089.
31. Messerschmidt, A., Prade, L., Kroes, S.J., Sanders-Loehr, J., Huber, R., and Canters, G.W., *Proc. Natl. Acad. Sci.*, 1998, vol. 95, no. 7, p. 3443.
32. Dodd, F.E., Van Beeumen, J., Eady, R.R., and Hasnain, S.S., *J. Mol. Biol.*, 1998, vol. 282, no. 2, p. 369.
33. Holland, P.L., and Tolman, W.B., *J. Am. Chem. Soc.*, 1999, vol. 121, no. 31, p. 7270.
34. Di Bilio, A.J., Chang, T.K., Malmstrom, B.G., Gray, H.B., Goran Karlsson, B., Nordling, M., Pascher, T., and Lundberg, L.G., *Inorg. Chim. Acta*, 1992, vols. 198--200, p. 145.
35. Gerdemann, C., Eicken, C., and Krebs, B., *Acc. Chem. Res.*, 2002, vol. 35, no. 3, p. 183.
36. Ferguson-Miller, S., and Babcock, G.T., *Chem. Rev.*, 1996, vol. 96, no. 7, p. 2889.
37. Zhou, Y.-H., Fu, H., Zhao, W.-X., Chen, W.-L., Su, C.-Y., Sun, H., Ji, L.-N., and Mao, Z.-W., *Inorg. Chem.*, 2007, vol. 46, no. 3, p. 734.
38. Bertini, I., Drago, R.S., and Luchinat, C., *The Coordination Chemistry of Metalloenzymes: The Role of Metals in Reactions Involving Water, Dioxygen and Related Species,* Springer, 2012.
39. Karlin, K.D., and Tyeklar, Z., *Bioinorganic Chemistry of Copper*, Springer, 2012.
40. Stubbe, J., and van der Donk, W.A., *Chem. Rev.*, 1998, vol. 98, no. 2, p. 705.
41. Murray, J.M., Saysell, C.G., Wilmot, C.M., Tambyrajah, W.S., Jaeger, J., Knowles, P.F., Phillips, S.E.V., and McPherson, M.J., *Biochemistry*, 1999, vol. 38, no. 26, p. 8217.
42. Knowles, P.F., Brown, R.D., Koenig, S.H., Wang, S., Scott, R.A., McGuirl, M.A., Brown, D.E., and Dooley, D.M., *Inorg. Chem.*, 1995, vol. 34, no. 15, p. 3895.
43. Peive, Ya. V. *Mikroelementy v sel'skom khozyaistve i meditsine* (Trace Elements in Agriculture and Medicine), Ulan-Ude: Buryatsk. Knizhn. Izd., 1968.
44. Takahashi, K., and Klinman, J.P., Biochemistry, 2006, vol. 45, no. 14, p. 4683.
45. Dooley, D.M., Scott, R.A., Knowles, P.F., Colangelo, C.M., McGuirl, M.A., and Brown, D.E., *J. Am. Chem. Soc.*, 1998, vol. 120, no. 11, p. 2599.
46. Gonzalo, G.D., Pazmino, D.E.T., Ottolina, G., Fraaije, M.W., and Carrea, G., *Tetrahedron: Asymmetry*, 2005, vol. 16, no. 18, p. 3077.
47. Pazmino, D.E., Winkler, M., Glieder, A., and Fraaije, M.W., *J. Biotechnol.*, 2010, vol. 146, nos. 1–2, p. 9.
48. Murrell, J.C., McDonald, I.R., and Gilbert, B., *Trends Microbiol.*, 2000, vol. 8, no. 5, p. 221.
49. Semrau, J.D., DiSpirito, A.A., and Yoon, S., *FEMS Microbiol. Rev.*, 2010, vol. 34, p. 496.
50. Lieberman, R.L., and Rosenzweig, A.C., *Crit. Rev. Biochem. Mol. Biol.*, 2004, vol. 39, no. 3, p. 147.
51. Steiner, R.A., Meyer-Klaucke, W., and Dijkstra, B.W., *Biochemistry*, 2002, vol. 41, no. 25, p. 7963.
52. Fusetti, F., Schroter, K.H., Steiner, R.A., van Noort, P.I., Pijning, T., Rozeboom, H.J., Kalk, K.H., Egmond, M.R., and Dijkstra, B.W., *Structure*, 2002, vol. 10, no. 2, p. 259.
53. Steiner, R.A., Kalk, K.H., and Dijkstra, B.W., *Proc. Natl. Acad. Sci. U. S. A.*, 2002, vol. 99, no. 26, p. 16625.
54. Reinhard, H., Kappl, R., Huettermann, J., and Viezzoli, M.-S., *J. Phys. Chem.*, 1994, vol. 98, no. 35, p. 8806.
55. Szilagyi, I., Labadi, I., Hernadi, K., Palinko, I., Fekete, I., Korecz, L., Rockenbauer, A., and Kiss, T., *New J. Chem.*, 2005, vol. 29, no. 5, p. 740.
56. Getzoff, E.D., Tainer, J.A., Stempien, M.M., Bell, G.I., and Hallewell, R.A., *Proteins: Struct., Funct., Bioinf.*, 1989, vol. 5, no. 4, p. 322.
57. McCord, J.M., and Fridovich, I., *J. Biol. Chem.*, 1969, vol. 244, no. 22, p. 6049.
58. Ohtsu, H., Shimazaki, Y., Odani, A., Yamauchi, O., Mori, W., Itoh, S., and Fukuzumi, S., *J. Am. Chem. Soc.*, 2000, vol. 122, no. 24, p. 5733.
59. Fukuzumi, S., Patz, M., Suenobu, T., Kuwahara, Y., and Itoh, S., *J. Am. Chem. Soc.*, 1999, vol. 121, no. 7, p. 1605.
60. Jiang, W., Han, Y., Pan, Q., Shen, T., and Liu, C., *J. Inorg. Biochem.*, 2007, vol. 101, no. 4, p. 667.
61. Lewis, E.A., and Tolman, W.B., *Chem. Rev.*, 2004, vol. 104, no. 2, p. 1047.

62. Mirica, L.M., Rudd, D.J., Vance, M.A., Solomon, E.I., Hodgson, K.O., Hedman, B., and Stack, T.D.P., *J. Am. Chem. Soc.*, 2006, vol. 128, no. 8, p. 2654.
63. Mirica, L.M., Vance, M., Rudd, D.J., Hedman, B., Hodgson, K.O., Solomon, E.I., and Stack, T.D.P., *J. Am. Chem. Soc.*, 2002, vol. 124, no. 32, p. 9332.
64. Palavicini, S., Granata, A., Monzani, E., and Casella, L., *J. Am. Chem. Soc.*, 2005, vol. 127, no. 51, p. 18031.
65. Sotomayor, M.D.P.T., Tanaka, A.A., and Kubota, L.T., *Electrochim. Acta*, 2003, vol. 48, no. 7, p. 855.
66. Fontecave, M., and Pierre, J.-L., *Coord. Chem. Rev.*, 1998, vol. 170, no. 1, p. 125.
67. Ramadan, A.E.-M. M., Ibrahim, M. M., and Shaban, S. Y., *J. Mol. Struct.*, 2011, vol. 1006, nos. 1–3, p. 348.
68. Bubacco, L., van Gastel, M., Groenen, E.J.J., Vijgenboom, E., and Canters, G.W., *J. Biol. Chem.*, 2003, vol. 278, no. 9, p. 7381.
69. Solomon, E.I., Baldwin, M.J., and Lowery, M.D., *Chem. Rev.*, 1992, vol. 92, no. 4, p. 521.
70. Tommerdahl, A.P., Burnett, K.G., and Burnett, L.E., *Biol. Bull.*, 2015, vol. 228, no. 3, p. 242.
71. Casella, L., Carugo, O., Gullotti, M., Garofani, S., and Zanello, P., *Inorg. Chem.*, 1993, vol. 32, no. 10, p. 2056.
72. Monzani, E., Quinti, L., Perotti, A., Casella, L., Gullotti, M., Randaccio, L., Geremia, S., Nardin, G., Faleschini, P., and Tabbi, G., *Inorg. Chem.*, 1998, vol. 37, no. 3, p. 553.
73. Fernandes, C., Neves, A., Bortoluzzi, A.J., Mangrich, A.S., Rentschler, E., Szpoganicz, B., and Schwingel, E., *Inorg. Chim. Acta*, 2001, vol. 320, nos. 1–2, p. 12.
74. Santhanam, N., Vivanco, J.M., Decker, S.R., and Reardon, K.F., *Trends Biotechnol.*, 2011, vol. 29, no. 10, p. 480.
75. Strong, P.J., and Claus, H., *Crit. Rev. Environ. Sci. Technol.*, 2011, vol. 41, no. 4, p. 373.
76. Thurston, C.F., *Microbiology*, 1994, vol. 140, no. 1, p. 19.
77. Madhavi, V., and Lele, S.S., *Bioresources*, 2009, vol. 4, p. 1694.
78. Gorbacheva, M.A., Shumakovich, G.P., Morozova, O.V., Strel'tsov, A.V., Zaitseva, E.A., and Shleev, S.V., *Moscow Univ. Chem. Bull. (Engl. Transl.)*, 2008, vol. 63, no. 2, p. 94.
79. *Lignocellulose Biotechnology: Future Prospects*, Kuhad, R.C., and Singh, A., Eds., Int. Publ. House, 2007.
80. d'Acunzo, F., Galli, C., and Masci., B., *Eur. J. Biochem.*, 2002, vol. 269, no. 21, p. 5330.
81. Lu, R., and Miyakoshi, T., *Enzyme Res.*, 2012, vol. 2012.
82. Lee, M.H., and Dawson, C.R., *J. Biol. Chem.*, 1973, vol. 248, no. 19, p. 6603.
83. Reinhammar, B., Aasa, R., Vänngård, T., Maritano, S., and Marchesini, A., *Biochim. Biophys. Acta, Protein Struct. Mol. Enzymol.*, 1997, vol. 1337, no. 2, p. 191.
84. Semenovich, M.S., *Fiziologiya rastenii* (Plant Physiology), St. Petersburg: BKhV-Peterburg, 2012.
85. Berezov, T.T. and Korovkin, B.F., *Biologicheskaya khimiya* (Biological Chemistry), Moscow: Meditsina, 1998.
86. Metzler, D.E., *Biochemistry: The Chemical Reactions of Living Cells*, Academic, 1973, 2nd ed.
87. Kubiak, T., Krzyminiewski, R., and Dobosz, B., *Curr. Top. Biophys.,* 2013, vol. 36, p. 7.
88. Vashchenko, V.I. and Vashchenko, T.N., *Psikhofarmakol. boil. narkol.*, 2006, vol. 6, no. 3, p. 1254.
89. Santagostini, L., Gullotti, M., Pagliarin, R., Bianchi, E., Casella, L., and Monzani, E., *Tetrahedron: Asymmetry*, 1999, vol. 10, no. 2, p. 281.
90. Lopez-Sandoval, H., Contreras, R., Escuer, A., Vicente, R., Bernes, S., Noth, H., Jeffery Leigh, G., and Barba-Behrens, N., *J. Chem. Soc., Dalton Trans.*, 2002, no. 13, p. 2648.
91. Adams, H., Bailey, N.A., Dwyer, M.J.S., Fenton, D.E., Hellier, P.C., Hempstead, P.D., and Latour, J.M., *J. Chem. Soc., Dalton Trans.*, 1993, no. 8, p. 1207.
92. Mukherjee, A., Rudra, I., Naik, S.G., Ramasesha, S., Nethaji, M., and Chakravarty, A.R., *Inorg. Chem.*, 2003, vol. 42, no. 18, p. 5660.
93. Gupta, S., Mukherjee, A., Nethaji, M., and Chakravarty, A.R., *Polyhedron*, 2004, vol. 23, no. 4, p. 643.
94. Rammal, W., Belle, C., Beguin, C., Duboc, C., Philouze, C., Pierre, J.-L., Le Pape, L., Bertaina, S., Saint-Aman, E., and Torelli, S., *Inorg. Chem.*, 2006, vol. 45, no. 25, p. 10355.
95. Tolman, W., *J. Biol. Inorg. Chem.*, 2006, vol. 11, no. 3, p. 261.
96. Zickermann, V., Verkhovsky, M., Morgan, J., Wikstrom, M., Anemuller, S., Bill, E., Steffens, G.C.M., and Ludwig, B., *Eur. J. Biochem.*, 1995, vol. 234, no. 2, p. 686.
97. Koutsoupakis, C., Soulimane, T., and Varotsis, C., *J. Am. Chem. Soc.*, 2003, vol. 125, no. 48, p. 14728.
98. Liu, J.-G., Naruta, Y., and Tani, F., *Chem. - Eur. J.*, 2007, vol. 13, no. 22, p. 6365.
99. Kamachi, T., Kihara, N., Shiota, Y., and Yoshizawa, K., *Inorg. Chem.*, 2005, vol. 44, no. 12, p. 4226.
100. Haltia, T., Brown, K., Tegoni, M., Cambillau, C., Saraste, M., Mattila, K., and Djinovic-Carugo, K., *Biochem. J.*, 2003, vol. 369, pt. 1, p. 77.
101. Lee, D.-H., Hatcher, L.Q., Vance, M.A., Sarangi, R., Milligan, A.E., Narducci Sarjeant, A.A., Incarvito, C.D., Rheingold, A.L., Hodgson, K.O., Hedman, B., Solomon, E.I., and Karlin, K.D., *Inorg Chem.*, 2007, vol. 46, no. 15, p. 6056.

102. Kapoor, A., Shandilya, M., and Kundu, S., *PLoS ONE*, 2011, vol. 6, no. 10.
103. Maiti, D., Woertink, J.S., Vance, M.A., Milligan, A.E., Narducci Sarjeant, A.A., Solomon, E.I., and Karlin, K.D., *J. Am. Chem. Soc.*, 2007, vol. 129, no. 28, p. 8882.
104. Brown, K., Djinovic-Carugo, K., Haltia, T., Cabrito, I., Saraste, M., Moura, J.G., Moura, I., Tegoni, M., and Cambillau, C., *J. Biol. Chem.*, 2000, vol. 275, no. 52, p. 41133.
105. Rasmussen, T., Berks, B.C., Butt, J.N., and Thomson, A.J., *Biochem. J.*, 2002, vol. 364, pt. 3, p. 807.
106. Brown, E.C., Bar-Nahum, I., York, J.T., Aboelella, N.W., and Tolman, W.B., *Inorg. Chem.*, 2007, vol. 46, no. 2, p. 486.
107. Gorelsky, S.I., Ghosh, S., and Solomon, E.I., *J. Am. Chem. Soc.*, 2006, vol. 128, no. 1, p. 278.
108. Yang, L., *PhD Thesis*, Norman, OK: Univ. Oklahoma, 2008.
109. McMaster, J., *Annu. Rep. Prog. Chem., Sect. A: Inorg. Chem.*, 2007, vol. 103, p. 492.
110. Oganesyan, V.S., Rasmussen, T., Fairhurst, S., and Thomson, A.J., *Dalton Trans.*, 2004, no. 7, p. 996.
111. Collman, J.P., Sunderland, C.J., Berg, K.E., Vance, M.A., and Solomon, E.I., *J. Am. Chem. Soc.*, 2003, vol. 125, no. 22, p. 6648.
112. Collman, J.P., Rapta, M., Broring, M., Raptova, L., Schwenninger, R., Boitrel, B., Fu, L., and L'Her, M., *J. Am. Chem. Soc.*, 1999, vol. 121, no. 6, p. 1387.
113. Collman, J.P., Boulatov, R., Sunderland, C.J., and Fu, L., *Chem. Rev.*, 2004, vol. 104, no. 2, p. 561.
114. Collman, J.P., Herrmann, P.C., Boitrel, B., Zhang, X., Eberspacher, T.A., Fu, L., Wang, J., Rousseau, D.L., and Williams, E.R., *J. Am. Chem. Soc.*, 1994, vol. 116, no. 21, p. 9783.
115. York, J.T., Bar-Nahum, I., and Tolman, W.B., *Inorg. Chim. Acta*, 2008, vol. 361, no. 4, p. 885.
116. Majouga, A.G., Beloglazkina, E.K., Moiseeva, A.A., Shilova, O.V., Manzheliy, E.A., Lebedeva, M.A., Davies, E.S., Khlobystov, A.N., and Zyk, N.V., *Dalton Trans.*, 2013, vol. 42, no. 18, p. 6290.
117. York, J.T., Bar-Nahum, I., and Tolman, W.B., *Inorg. Chem.*, 2007, vol. 46, no. 20, p. 8105.
118. Lee, Y., Sarjeant, A.A.N., and Karlin, K.D., *Chem. Commun.*, 2006, no. 6, p. 621.
119. Brown, E.C., York, J.T., Antholine, W.E., Ruiz, E., Alvarez, S., and Tolman, W.B., *J. Am. Chem. Soc.*, 2005, vol. 127, no. 40, p. 13752.

Translated by D. Zvukov